LUND UNIVERSITY

Exploring the miRNA profile of medium spiny neurons using retrograde transport in rats

Lockowandt, Marcus

2021

Document Version:
Publisher's PDF, also known as Version of record

Exploring the miRNA profile of medium spiny neurons using retrograde transport in rats

Marcus Lockowandt

LUND
UNIVERSITY

DOCTORAL DISSERTATION

by due permission of the Faculty of Medicine, Lund University, Sweden.
To be defended at Segerfalksalen, Wallenberg Neuroscience Centre, Lund, Sweden, at 13:00 on the 4th of June 2021.

Faculty opponent
Professor Thomas Juhl Corydon

Department of Biomedicine, Aarhus University, Denmark

Organization	Document name
LUND UNIVERSITY CNS Gene Therapy, Department of Experimental Medical Science, Faculty of Medicine, Lund University, Sweden	**DOCTORAL DISSERTATION**
	Date of issue 2021-06-04
Author(s) Marcus Lockowandt	Sponsoring organization

Title and subtitle
Exploring the miRNA profile of medium spiny neurons using retrograde transport in rats

Abstract

The basal ganglia play an essential role in movement selection and control. It is therefore not surprising that they are central to neurodegenerative diseases like Parkinson's disease and Huntington's disease. As such, greater knowledge of how the different parts of the basal ganglia behave, both in their normal and in disease states, will increase our understanding of the system and help in finding new and improved ways to treat the possible disorders.

In this thesis we were interested in the starting point of the basal ganglia, the medium spiny neurons of the striatum. Generally categorized into two groups, the direct pathway medium spiny neurons, projecting to the substantia nigra and responsible for activating action, and the indirect pathway medium spiny neurons, projecting to the globus pallidus and responsible for inhibiting action. We were interested in exploring their respective miRNA profiles to find if there were large differences to be found there. MiRNA are short RNA, around 22 nt in length that function as guides for the RNA-induced silencing complex to downregulate protein expression.

Through the expression of a fusion-protein composed of one of the components of the RNA-induced silencing complex responsible for miRNA binding, and GFP, it is possible to isolate the miRNA populations of cells expressing this fusion-protein. We injected virus, expressing the fusion-protein and capable of retrograde transport, into these areas. We were able to show that both a lentivirus containing a rabies virus fusion envelope, and an adeno-associated virus with a modified AAV2 capsid could be used for this purpose. Following successful transduction of cells in the striatum by retrograde transport, miRNA was sequenced and compared between the two populations. In total eight different miRNA were found to be differentially expressed between them. One of which had simultaneously also been identified by another group using a different set of methods in mice. Finally, we also explore the expression profile of a dopamine receptor D2 specific promoter element within the dorsal striatum.

Key words
miRAP, miRNA, medium spiny neurons, retrograde transport, FuGB

Classification system and/or index terms (if any)

Supplementary bibliographical information		**Language** English
ISSN and key title 1652-8220		**ISBN** 978-91-8021-060-7
Recipient's notes	**Number of pages** 142	Price
	Security classification	

Signature 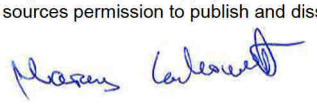 Date 2021-04-27

Exploring the miRNA profile of medium spiny neurons using retrograde transport in rats

Marcus Lockowandt

2021

LUND
UNIVERSITY

CNS Gene Therapy
Department of Experimental Medical Science
Faculty of Medicine
Lund University

Coverphoto by Marcus Lockowandt

Faculty of Medicine
Department of Experimental Medical Science

ISBN 978-91-8021-060-7
ISSN 1652-8220

Printed in Sweden by Media-Tryck, Lund University
Lund 2021

Table of Contents

Original papers and manuscripts

Paper I
Optimization of production and transgene expression of a retrogradely transported pseudotyped lentiviral vector.
Lockowandt M., Günther D. M., Quintino L., Breger L. S., Isaksson C., Lundberg C.
J Neurosci Methods, 2020. 336: p. 108542.

Paper II
A comparison of AAV-vector production methods for gene therapy and preclinical assessment.
Davidsson M., Negrini M., Hauser S., Svanbergsson A., **Lockowandt M.**, Tomasello G., Manfredsson F. P., Heuer A.
Scientific Reports, (2020) 10:21532.

Paper III
Exploring the miRNA populations of medium spiny neurons of the striatum through the use of retrograde transport.
Lockowandt M., Garza R., Quintino L, Johansson J.G., Jakobsson J., Lundberg C.
Manuscript 2021

Paper IV
Determining the specificity of the DRD2 specific promoter in the dorsal striatum
Lockowandt M., Lundberg C.
Manuscript 2021

Abstract

The basal ganglia play an essential role in movement selection and control. It is therefore not surprising that they are central to neurodegenerative diseases like Parkinson's disease and Huntington's disease. As such, greater knowledge of how the different parts of the basal ganglia behave, both in their normal and in disease states, will increase our understanding of the system and help in finding new and improved ways to treat the possible disorders.

In this thesis we were interested in the starting point of the basal ganglia, the medium spiny neurons of the striatum. Generally categorized into two groups, the direct pathway medium spiny neurons, projecting to the substantia nigra and responsible for activating action, and the indirect pathway medium spiny neurons, projecting to the globus pallidus and responsible for inhibiting action. We were interested in exploring their respective miRNA profiles to find if there were large differences between the two. MiRNA are small ssRNAs, around 22 nt in length that function as guides for the RNA-induced silencing complex to downregulate protein expression.

Through the expression of a fusion-protein composed of one of the components of the RNA-induced silencing complex responsible for miRNA binding, and GFP, it is possible to isolate the miRNA populations of cells expressing this fusion-protein. We injected virus, expressing the fusion-protein and capable of retrograde transport, into these areas. We were able to show that both a lentivirus containing a rabies virus fusion envelope, and an adeno-associated virus with a modified AAV2 capsid could be used for this purpose. Following successful transduction of cells in the striatum by retrograde transport, miRNA was sequenced and compared between the two populations. In total eight different miRNA were found to be differentially expressed between them. One of which had simultaneously also been identified by another group using a different set of methods in mice. Finally, we also explore the expression profile of a dopamine receptor D2 specific promoter element within the dorsal striatum.

Populärvetenskaplig sammanfattning

De basala ganglierna är en grupp av områden i hjärnan som spelar en central roll för vår förmåga att utföra handlingar. Det är därför föga förvånande att sjukdomar som har en inverkan på deras funktion kan få långtgående negativa konsekvenser. Förutom neurodegenerativa sjukdomar såsom Parkinsons sjukdom och Huntingtons sjukdom, så är de basala ganglierna även involverade i neurologiska sjukdomar som Tourettes syndrom, Cerebral pares, OCD och Tardiv dyskinesi. Den stora mängden sjukdomar kopplade till dem basala ganglierna motiverar behovet av att öka förståelsen för hur de olika delarna av detta komplexa nätverk fungerar.

Det finns två kanaler längs vilken informationen flödar genom dem basala ganglierna, den direkta kanalen samt den indirekta kanalen. När informationen leds igenom dessa två olika kanaler så bearbetas och modifieras den beroende på tidigare erfarenheter, innan den slutligen leder till handling. De byggstenar som utgör dessa kanaler är nervceller, celler som är kapabla till att leda vidare och modifiera elektriska impulser. En signal tas emot i dendriterna, ett förgrenat nätverk av utskott från cellkroppen som andra nervceller kan ansluta till via sina axoner. Därifrån leds signalerna vidare till cellkroppen. Väl i cellkroppen så summeras signalerna från alla dendriter och leder antingen till att en signal skickas vidare längs axonen till nästa cell, eller till att ingenting händer. Dessa axoner kan vara väldigt långa och tillåter en nervcell som har sina dendriter och sin cellkropp i en del av hjärnan, att skicka signaler till en helt annan del av hjärnan. Den direkta samt den indirekta kanalen tar sin början i en del av hjärnan som kallas striatum. Härifrån skickar neuroner sina axoner antingen till substantia nigra om de tillhör den direkta kanalen, eller till globus pallidus om de tillhör den indirekta kanalen.

Det finns vissa virus som kan infektera nervceller via deras axoner och sedan transporteras tillbaka till cellkroppen längs dessa. Genom att injicera ett sådant virus antingen i substantia nigra eller i globus pallidus, så kan vi infektera nervceller som tillhör endast den direkta eller indirekta kanalen. Nervceller som blir infekterade av viruset uttrycker ett protein, Argonaute2 som binder till en specifik typ av RNA som kallas för microRNA (miRNA). Vi kan sedan fiska ut detta protein från krossade celler tillsammans med miRNAt från de infekterade cellerna. Det finns många olika typer av

miRNA som förekommer i olika kvantiteter i olika celler. De tillåter celler att modifiera uttryck av protein och spelar en viktig roll för att cellerna ska fungera korrekt.

I denna avhandling så har vi bekräftat att ett specifikt virus kan användas för att infektera nervceller från striatum som tillhör den direkta eller indirekta kanalen genom injektion i globus pallidus eller substantia nigra. Vi har modifierat viruset med hjälp av väl etablerade metoder för att få de infekterade neuronerna att uttrycka proteinet Argonaute2. Med hjälp av det modifierade viruset har vi sedan lyckats extrahera miRNA från dessa två typer av nervceller. Vi har sedan kvantifierat de olika typerna av miRNA och jämfört vilka skillnader som förekommer i mängderna av specifika miRNA beroende på injektionsställe. Totalt har vi lyckats identifiera åtta olika miRNA som förekommer i olika mängder mellan de två typerna av striatala neuroner. En av dessa miRNA, miR-126a-3p har även identifierats av en annan grupp som studerat miRNA från samma celler med en annan metod. Vi hoppas att i framtiden kunna utforska de protein som är reglerade av dessa miRNA, samt kunna studera skillnader i sjukdomsmodeller.

Lay summary

The basal ganglia are a collection of areas in the brain that play a central role in our ability to take actions. It is therefore not surprising that diseases that have an impact on their function can have far-reaching negative consequences. In addition to neurodegenerative diseases such as Parkinson's disease and Huntington's disease, the basal ganglia are also involved in neurological diseases such as Tourette's syndrome, Cerebral palsy, OCD and Tardive dyskinesia. The large number of diseases linked to the basal ganglia show why there is a need to increase understanding of how the various parts of this complex network functions.

There are two pathways along which the information flows through the basal ganglia, the direct pathway and the indirect pathway. When the information is passed through these two different channels, it is processed and modified in a manner dependent upon previous experience, before it finally leads to action. The building blocks that make up these channels are neurons, cells that can conduct and modify electrical impulses. A signal is received in the dendrites, a branched network of protrusions from the cell body that other neurons can connect to via their axons. From there, the signals are passed on to the cell body. Once in the cell body, the signals from all dendrites are aggregated and lead either to a signal being passed along the axon to the next cell, or to nothing happening. These axons can be very long and allow a neuron that has its dendrites and its cell body in one part of the brain, to send signals to a completely different part of the brain. The direct as well as the indirect pathway start in a part of the brain called the striatum. From here, neurons send their axons either to the substantia nigra if they belong to the direct pathway, or to the globus pallidus if they belong to the indirect pathway.

There are some viruses that can infect neurons at the end of their axons and then move back to the cell body through the axons. By injecting such a virus either into the substantia nigra or into the globus pallidus, we can infect neurons that belong to the direct or indirect pathway. Neurons that become infected by the virus express a protein, Argonaute2, that binds to a specific type of RNA called microRNA (miRNA). We can then fish out this protein from homogenized cells along with the miRNA from the infected cells. There are many different types of miRNAs that occur in different

quantities in different cells. They allow cells to modify the expression of proteins and play an important role in the proper functioning of the cells.

In this dissertation, we have confirmed that a specific virus can be used to infect neurons from the striatum, that belong to the direct or indirect pathway, by injection into the globus pallidus or substantia nigra. We have modified this virus using well-established methods to get the infected neurons to express the protein Argonaute2. With the help of the modified virus, we succeeded in extracting miRNA from these two types of neurons. Following extraction, we quantified the different types of miRNAs, and compared the differences following injection into either the substantia nigra or the globus pallidus. We successfully identified eight different miRNAs that occur in different amounts between the two types of striatal neurons. One of these miRNAs has also been identified as being differently expressed by another group that studied the same cells using a different method. We hope these findings can be employed to take a closer look at the proteins targeted and to look at differences in disease models.

Abbreviations

AAV	adeno-associated virus
AGO	argonaute
BG	basal ganglia
BSA	Bovine serum albumin
ChAT	Choline acetyltransferase
Chl	Chloroform purification
CP	caudoputamen
CSF	Cerebrospinal fluid
D2SP	Dopamine receptor D2 specific promoter
DE	differentiial expression
dMSN	direct pathway medium spiny neuron
DRD1	dopamine receptor D1
DRD2	dopamine receptor D2
EP	entopeduncular nucleus
FACS	fluorescence-activated cell sorting
FuG-B	Fusion glycoprotein B
GABA	gamma-aminobutyric acid
GFP	green fluorescent protein
GP	globus pallidus
GPi	globus pallidus internal
HD	Huntingotn's disease
HIV	human immunodeficiency virus
hSyn	human Synapsin
iMSN	indirect pathway medium spiny neuron
Iod	Iodixanol purification
ITR	inverted terminal repeat
L-Dopa	Levodopa
LID	Levodopa induced dyskinesia
LMD	Laser microdissection
LV	lentivirus
miRAP	miRNA affinity purification

miRNA	micro RNA
mRNA	messenger RNA
MSN	medium spiny neuron
MWCO	Molecular weight cut-off
Nac	nucleus accumbens
NDD	Neurodegenerative disorders
PD	Parkinson's disease
PEI	Polyethyleneimine
pre-miRNA	precursor micro RNA
pri-miRNA	primary micro RNA
rAAV	recombinant adeno-associated virus
RISC	RNA-induced silencing complex
RNA-seq	RNA sequencing
RT-qPCR	Reverse transcriptase quantitative PCR
SIN	self-inactivating
SNpc	substantia nigra pars compacta
SNpr	substantia nigra pars reticulata
STN	subthalamic nucleus
TH	Tyrosine hydroxylase
VSV	vesicular stomatitis virus
VSV-G	vesicular stomatitis virus glycoprotein
wt	wildtype
RT	room temperature
O/N	over night

Introduction

A very brief introduction to the basal ganglia

The basal ganglia (BG) play an essential role in movement selection and control. They consist of a network of subcortical nuclei including the striatum (caudoputamen (CP) and nucleus accumbens (Nac) in rats), the globus pallidus (GP), subthalamic nucleus (STN) and the substantia nigra. The CP and Nac are thought to serve as input nuclei, receiving efferents from cortical and thalamic nuclei (McGeorge & Faull, 1989), as well as the substantia nigra pars compacta (SNpc), while the substantia nigra pars reticulata (SNpr) serves as an output nucleus primarily to the thalamus. The other nuclei are involved in processing the input information in order to deliver an output (Alexander & Crutcher, 1990). This basic and straightforward connection pattern in combination with information from different neuronal disorders led to the initial models of how movement and action selection worked (Albin, Young, & Penney, 1989; Alexander & Crutcher, 1990). While these models have served well in providing a very basic and somewhat simplified understanding of how the BG work, improved tools and increased knowledge, have yielded data that is not completely compatible with the original models. However, before we take a closer look at the models, we should briefly discuss the most numerous of the neurons of the BG (Oorschot, 1996). The neurons where it all starts; the medium spiny neurons of the striatum (MSN).

The medium spiny neurons of the striatum

There are multiple different ways to separate neurons. One might look at their morphological properties, their electrophysiological properties, their transcriptome/proteome, their location within the brain, where they send projections and whence they receive them. All these factors play a role in defining what larger group of neurons a single neuron belongs to. How we chose to define these groups should be dependent on the question we are trying to answer and the assumptions we are willing to make to answer that question. Do we believe that all the neurons projecting from one area to another is responsible for regulating behaviour in a specific manner? If so, it might make sense to group these neurons together based on where they project. An

example of this is the frequent grouping of all MSN into one of two groups. Either the dopamine receptor D1 (DRD1) positive MSN of the direct pathway (dMSN), or the dopamine receptor D2 (DRD2) positive MSN of the indirect pathway (iMSN). While morphologically highly similar, essentially completely intermingled in the striatum, and both inhibiting downstream targets through the release of gamma-aminobutyric acid (GABA), the two groups are different with regards to their electrophysiological properties, their transcriptome/proteome, and where they send projections.

The dMSN are characterized by a number of features. On the transcriptome/proteome level they are primarily differentiated from iMSN through their expression of DRD1, Adora1, dynorphin and substance P (Albin et al., 1989; Bateup et al., 2010; Gerfen et al., 1990; Gertler, Chan, & Surmeier, 2008; Gokce et al., 2016). They send projections terminating in the SNpr, but also send collaterals to the GP and entopeduncular nucleus (EP) (Cazorla et al., 2014; Fujiyama et al., 2011). Morphologically they can be distinguished by their increased dendritic length and total number of branch points compared to iMSN (Gertler et al., 2008). When it comes to their electrophysiological properties, dMSN have been found to be less excitable compared to iMSN, with Dopamine acting to increase dMSN excitability (Brown, Planert, Berger, & Silberberg, 2013; Gertler et al., 2008).

The iMSN on the other hand are defined by their expression of DRD2, Adora2a and enkephalin (Albin et al., 1989; Bateup et al., 2010; Gokce et al., 2016). They send projections to the neighbouring GP (Cazorla et al., 2014; Fujiyama et al., 2011) and Dopamine acts to inhibit their excitability (Hernández-López et al., 2000).

This division is made somewhat problematic by the presence of a population of DRD1/DRD2 double-positive population expressing both dynorphin and enkephalin detected through single-cell sequencing, co-labelling with antibodies, in situ hybridization and through labelling in transgenic mice with a fluorophore (George, O'Dowd, Hasbi, & Perreault, 2011; Perreault et al., 2010; Stanley, Gokce, Malenka, Sudhof, & Quake, 2020). Some have suggested that these cells contain D1-D2 heterodimers that activate G_q and by extension phospholipase C (Rashid et al., 2006). These heterodimers and their impact on behaviour has been further studied, primarily in the context of the Nac and the heterodimers' role in induction of depression- and anxiety-like behaviours (Hasbi et al., 2014; Shen et al., 2015) However, whether the D1-D2 heterodimers actually exist is contested with evidence both against (Frederick et al., 2015; S.-M. Lee et al., 2014) and in favour of the presence and functionality of a D1-D2 heterodimer (Hasbi et al., 2020; Perreault et al., 2010; Rashid et al., 2006). Regardless of whether a D1-D2 heterodimer exists or not, the presence of cells expressing both DRD1 and DRD2 has been detected through multiple different methods. The features of this population of neurons, referred to as D1H by Gokce *et*

al. (Gokce et al., 2016) has to the best of my knowledge not been explored separately from those of the DRD1 or DRD2-positive MSN within the caudate putamen. While some tracing and immunostaining studies have suggested that they are primarily dMSN (Deng, Lei, & Reiner, 2006), there have been no behavioural studies performed targeting specifically this population of neurons.

Most of the behavioural studies performed to date looking at the impact of activation of either the dMSN or iMSN employ the use of DRD1-Cre, DRD2-Cre or Adora2a-Cre transgenic mice (Bateup et al., 2010; Cui et al., 2013; Klaus, Alves da Silva, & Costa, 2019; J. Lee, Wang, & Sabatini, 2020; Nonomura et al., 2018) or modulate dopamine receptor signalling through the use of small molecules (Eilam & Szechtman, 1989; Ralph & Caine, 2005). These studies generally show that activation of DRD1-Cre or Tac1-Cre (a substance P precursor) neurons lead to increased movement, be it either through ambulation, AIMS test or an increase in contralateral rotations. On the other hand, activation of DRD2-Cre or Adora2a-Cre neurons generally lead to a decrease in movement (Alcacer et al., 2017; Bateup et al., 2010; Eilam & Szechtman, 1989; Kravitz et al., 2010; Ralph & Caine, 2005). These observations are in line with the "classical model" of the direct and indirect pathway (Figure 1) (Albin et al., 1989), according to which activation of the dMSN causes release of GABA, leading to inhibition of the SNpr neurons that are responsible for inhibition of the thalamo-cortical glutamatergic neurons. The release of glutamate from these thalamo-cortical neurons in turn lead to activation of locomotor action. Conversely, activation of the iMSN causes release of GABA at the GP, inhibiting the activity of GABAergic GP neurons projecting to the STN. This inhibition of the GABAergic GP neurons causes an increased release of glutamate from the STN neurons projecting to the SNpr, which in turn leads to increased inhibition of the thalamo-cortical glutamatergic neurons.

To simplify, activation of dMSN leads to an increase in thalamo-cortical stimulation, while activation of iMSN leads to a decrease in thalamo-cortical stimulation (Albin et al., 1989; Alexander & Crutcher, 1990).

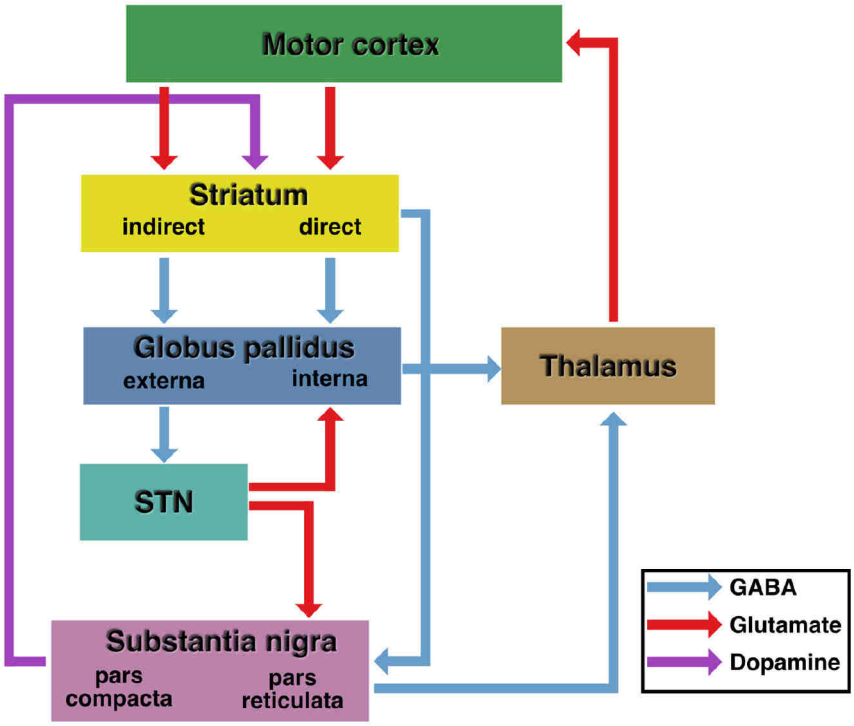

Figure 1: An illustration of the classical model of the basal ganglia. GABA-ergic neurons act to inhibit their target, while Glutamate acts in an excitatory fashion. The role of dopamine is dependent on the target, with dMSN generally being excited and iMSN inhibited by its release.Function of the dMSN, iMSN and the "classical model"

Updating the "classical model"

While the classical model, in broad strokes, holds up in terms of how the basal ganglia impacts action selection and seems relevant for the gross disruption of motor actions seen in some neurodegenerative disorders (DeLong & Wichmann, 2007; O'Callaghan, Bertoux, & Hornberger, 2013; Roos, 2010; Vonsattel et al., 1985), it is becoming clear that it does not properly describe the method by which the brain selects whether a specific action should be performed or not. Calcium imaging studies to observe neuronal activation in performing rodents (Cui et al., 2013; Jin, Tecuapetla, & Costa, 2014), indicate that both iMSN and dMSN are activated during initiation of actions. More recent studies (Nonomura et al., 2018; Tecuapetla, Jin, Lima, & Costa, 2016) further enforced the somewhat more complex manner in which the dMSN and iMSN

are suggested to influence action selection and movement. They suggest that instead of a general activation of dMSN initiating and maintaining movement, it seems that it is necessary to activate the right set of dMSN to promote the "correct" action, and to a lesser extent maintain it, while activating the correct iMSN to inhibit competing actions. Furthermore, the iMSN also seem to be responsible for switching to a different action when reward is absent rather than just universally downregulating movement. Not all research supports this model however (Ueda et al., 2017) and more than likely there is a lot of research left to be done before we can hope to completely understand how this complex part of the brain works.

Neurodegeneration and the basal ganglia

As the number of people that live past 60 continues to increase, so will the number of people whose lives are negatively impacted by neurodegenerative disorders (NDD). While there are a wide variety of disorders that are of importance when studying the striatum, we have chosen to briefly explore the two most common, and probably most well-known degenerative disorders, Parkinson's disease (PD) and Huntington's disease (HD).

Parkinson's Disease

PD is the second most common NDD after Alzheimer's disease, with approximately 1% of people aged 65 or above suffering from the disease (Wirdefeldt, Adami, Cole, Trichopoulos, & Mandel, 2011). PD is primarily characterized by tremors at rest, bradykinesia, postural instability and rigidity (Jankovic, 2008). In addition, non-motor symptoms such as cognitive decline, depression, visual hallucinations, apathy and anxiety can also occur (Meireles & Massano, 2012). The disease is caused by the gradual degeneration and death of dopaminergic neurons of the SNpc, which leads to a lack of dopamine innervation of the MSN of the direct and indirect pathway. PD is further split into familial and sporadic forms, with familial being caused by genetic mutations, while the sporadic form is caused by reasons not completely understood. The most widely accepted theory is that aggregation of specific proteins like alpha-synuclein, causes the death of the neurons with the exact cause for their aggregation not completely understood (Baba et al., 1998; Meireles & Massano, 2012). Occurrence of the sporadic form of PD has been linked to some external risk-factors such as exposure to pesticides, a high intake of dairy products, methamphetamine use and melanoma.

On the other hand, intake of coffee or tea, use of tobacco and physical activity was found to decrease the likelihood of PD (Baba et al., 1998).

The standard treatment of PD for decades has been Levodopa (L-DOPA), a precursor of dopamine that is taken up in the brain, converted to dopamine and then released (Lopez, Munoz, Guerra, & Labandeira-Garcia, 2001). However, this treatment has over time been complimented by Dopamine agonists, Monoamine oxidase-B inhibitors, Catechol O-methyltransferase inhibitors, Anticholinergics, Amantadines (Connolly & Lang, 2014) or deep brain stimulation of various nuclei like the STN, GP internal (GPi) and ventralis intermediate nucleus (Groiss, Wojtecki, Südmeyer, & Schnitzler, 2009). Eventually however L-DOPA stops being effective, and an unavoidable side effect of L-DOPA treatment is a disorder called Levodopa induced dyskinesia (LID). LID manifests as involuntary movements that occur associated with L-DOPA administration (Mercuri & Bernardi, 2005). Experiments on animal models have shown that LID involves dysregulation of the dopamine receptors present in direct and indirect pathway neurons and that restoring or counteracting this dysregulation can potentially help restore the pathways to a more normal state (Fieblinger et al., 2018; Santini, Heiman, Greengard, Valjent, & Fisone, 2009; Sebastianutto et al., 2020; Solis, Garcia-Montes, Gonzalez-Granillo, Xu, & Moratalla, 2015). Due to its negative impact on the patient's quality of life, it is important to improve our understanding of LID and to find ways to treat it.

Huntington's disease

Huntington's disease (HD) is another relatively well-known disease that occurs in roughly 1/10-20000 people among Caucasians. It's a genetic disorder inherited in an autosomal dominant manner with an age of onset typically between 30 and 50 years of age (Roos, 2010). Its symptoms include chorea (unwanted movements), motor impairment, apathy, irritability and dementia. HD is caused by an overabundance of CAG repeats within the huntingtin gene, with an increased CAG repeat length (>27) generally increasing penetrance and severity of the disease (Rosenblatt et al., 2012). These CAG repeats when present in too large numbers, are thought to increase the likelihood of the formation of aggregates of the cleaved huntingtin protein, which in turn leads to cell death starting with the MSN (Bates et al., 2015; Borchelt et al., 2012). While the number of CAG-repeats is the single largest risk factor, it does not completely explain the age of onset and penetrance of the disease and other genes have been suggested as potential risk factors (Gusella, MacDonald, & Lee, 2014).

There is no cure for HD and it eventually leads to the death of the patient. However, the symptoms can be managed to some degree. Treatments include tetrabenazine for

Chorea (Group, 2006) as well as physiotherapy to deal with some of the other minor motor-problems, like abnormal gait and poor balance. The neuropsychiatric symptoms are treated as they would be in other diseases, with depression often being treated either through cognitive behavioural therapy or through selective serotonin uptake inhibitors (Bates et al., 2015; McColgan & Tabrizi, 2018).

Viral vectors for gene therapy

Viral vectors serve as a great tool for delivery of genetic material to a wide range of different cells. They have evolved to efficiently transmit their own genetic material to different cell-types in order to hijack the cellular machinery for their own replication. Thanks to the tools of modern molecular biology, we can now hijack them in order to introduce the genetic material we see fit into cells, allowing for (in theory) an unparalleled level of control. This is done by replacing parts, or most of the viral genome, with the desired genetic material to be introduced into the target cells. The material necessary for viral replication is introduced to cells dissociated from the sequences that tells a virus what genetic material to transport. Thus, the virus can replicate within these cells, however the virus generated is incapable of replication, since it lacks the necessary proteins to do so. We used two different types of viruses that are widely used for gene therapy, lentivirus (LV) and adeno-associated virus (AAV).

Lentivirus

The LV commonly used today in gene therapy is a modified version of the Human immunodeficiency virus (HIV)-1 (Dull et al., 1998; Naldini et al., 1996; Poznansky, Lever, Bergeron, Haseltine, & Sodroski, 1991; Salmon & Trono, 2007; Trono, 2000). HIV is a retrovirus that is responsible for causing acquired immune deficiency syndrome through infection of the $CD4^+$ T-cells and Macrophages, severely disrupting the immune-system which eventually leads to the death of the patient through other diseases. At its peak, HIV caused approximately 2.4 million deaths worldwide in 2005, but due to an increase in treatment with anti-retroviral drugs, these numbers have gone down (Deeks, Overbaugh, Phillips, & Buchbinder, 2015).

The virus consists of a single-stranded positive sense RNA which in the wildtype carries the genes *gag*, *pol*, *env*, *rev*, *tat*, *vif*, *vpr*, *vpu* and *nef*. The first generation of lentiviral vectors retained all of these proteins for the production of recombinant LV with the exception of the *env* gene which was instead originally replaced with the envelope protein from vesicular stomatitis virus (VSV). The VSV envelope protein allowed for

transduction of a greater number of different types of cells due to interacting with the Low density lipo-protein receptor (Nikolic et al., 2018), as well as improving stability of the viral particle to allow for purification using ultra-centrifugation. In order to increase safety and prevent the creation of a replication competent virus through recombination, production was performed using one plasmid for expression of the envelope (envelope plasmid), one for the viral proteins (packaging plasmid) and a third one containing the viral genome (transfer plasmid) to be delivered into the cells (Naldini et al., 1996). Of these three plasmids, only the transfer plasmid possessed the original 5' and 3' LTRs, while the envelope and packaging plasmids relied on the CMV promotor and a poly-A tail for transcription of messenger RNA (mRNA). These viruses were found to be able to transduce neurons (Naldini et al., 1996), muscle (Kafri, Blömer, Peterson, Gage, & Verma, 1997) and liver (Kafri et al., 1997).

The second generation of LVs saw the removal of the genes *vif*, *vpr*, *vpu* and *nef* as these genes are not necessary for the transduction of most cell lines, or the production of LVs in the HEK293 or HEK293T cell-line (Romain Zufferey, Nagy, Mandel, Naldini, & Trono, 1997). To further improve the safety of the recombinant LVs, modifications were made to the 3' U3 sequence of the transfer plasmid. The 5' U3 sequence hosts the transcription start site for the viral genome once integrated into the host genome. Thus, in order for a virus-particle to be able to multiply, it needs a functional 5' transcription start site to replicate the virus-proteins and genome. The reason that the 3' U3 sequence was changed, is that during reverse transcription of the viral RNA into a double-stranded DNA, the 3' U3 sequence serves as template to create the 5' U3 sequence (Hu & Hughes, 2012; R. Zufferey et al., 1998). In our LV production we have used a second generation packaging systems with self-inactivating (SIN) transfer plasmids, however, especially for the purpose of production of LVs aimed at a clinical setting, a third generation LV production system is available which offers even greater safety (Dull et al., 1998). The third-generation system replaces the 5' U3 sequence of the transfer plasmid LTR with another promoter element such as one from CMV or Rous sarcoma virus, removes the *tat* gene, and moves *rev* onto a second packaging plasmid. All these changes serve to reduce the likelihood of recombination into a replication competent virus, without a major negative impact on transduction efficiency (Dull et al., 1998).

Fusion glycoprotein

As mentioned before, LVs today are frequently pseudotyped with the VSV glycoprotein (VSV-G) (Joglekar & Sandoval, 2017). This envelope protein has a broad tropism due to its receptor being available on most cell types (Nikolic et al., 2018), but many other

envelope proteins have been used (Joglekar & Sandoval, 2017), often to target a specific cell-type. Because we were looking to transduce MSN based on whether they were projecting to the GP or SNpr, we were looking for an envelope which would allow our lentivirus to be retrogradely transported. A modified version of the Rabies virus glycoprotein was published around 2011. This modified version, called fusion glycoprotein B (FuG-B), is a fusion of the transmembrane domain of the Vesicular stomatitis virus glycoprotein and the extracellular domain of the Rabies virus glycoprotein. This glycoprotein is capable of being transported retrogradely by neurons like the Rabies virus glycoprotein while yielding higher titers in viral production (Hirano et al., 2013; Kato, Kobayashi, et al., 2011; Kato, Kuramochi, et al., 2011). FuG-B, composed of the extracellular and transmembrane domain of the challenge virus standard strain passaged in suckling mouse brain (Morimoto et al., 1998) as well as the intracellular membrane of VSV-G was the first version developed and tested. Of the different envelope configurations tested, it was found to be the most efficient both for generating higher titers and for transducing neurons in vivo (Kato, Kobayashi, et al., 2011). A second version of the envelope was later published with the same configuration of domains, but instead based on the Pasteur virus strain of the rabies virus (Kato, Kuramochi, et al., 2011). This envelope, termed FuG-B2, showed slightly higher titers compared to FuG-B.

Adeno associated virus

AAV is a small (roughly 22 nm) single strand DNA virus. It was discovered in 1965 as part of Adenovirus preparations (Atchison, Casto, & Hammon, 1965; Hoggan, Blacklow, & Rowe, 1966). It consists of a single DNA strand which contains the *rep*, *aap*, and *cap* genes (Lusby, Fife, & Berns, 1980). *Cap* codes for the capsid proteins VP1, VP2 and VP3 which together make up the capsid surrounding the viral genome (Wistuba, Kern, Weger, Grimm, & Kleinschmidt, 1997). There are several different wildtype capsid proteins, as well as a large number of engineered capsids, with modifications usually intended to change tropism, susceptibility to antibodies, retrograde transport, ability to cross the blood-brain-barrier, etc. The *aap* gene codes for the assembly-activating protein which is involved in capsid assembly (Sonntag et al., 2011). While *rep* codes for the proteins Rep40, 52, 68, and 78 which play an integral role in viral replication. Rep 40 and 52 are thought to be responsible for packaging of the viral genome into the assembled capsid (King, 2001), while 68 and 78 are essential to viral genome replication and integration (Bardelli et al., 2016; R. Jude Samulski & Muzyczka, 2014). Not all proteins needed for viral replication are however found in the AAV genome. As a member of the *Dependoparvovirus* genus, AAV replication is greatly enhanced in the presence of other helper-viruses (Nash,

Chen, & Muzyczka, 2008). The two most studied helper viruses are probably Adenoviruses type 5 and Herpes simplex virus type 1, although other viruses are also known to serve as helper viruses (Meier, Fraefel, & Seyffert, 2020).

For the purposes of production of recombinant AAVs (rAAV) the Adenoviral proteins E1, E4, E2a, and VA are commonly used as helper virus proteins (Meier et al., 2020; Xiao, Li, & Samulski, 1998). They are used in addition to the previously mentioned *rep, cap* and *aap* proteins. E1 is present in HEK293 cells already and so does not need to be added in the helper plasmid for rAAV production in this commonly used cell-line. These helper proteins are involved in initiation of transcription of Rep proteins (Chang, Shi, & Shenk, 1989), exporting of viral mRNA (Pilder, Moore, Logan, & Shenk, 1986), replication of viral DNA (Stracker et al., 2004), and inhibition of protein kinase R to prevent degradation of AAV proteins (Nayak & Pintel, 2007). Similarly to the process of LV production, the desired transgene construct is inserted between two inverted terminal repeats (ITR) as part of the transfer plasmid. The ITRs serve as a necessary motif for replication of the viral genome due to their ability to form a hairpin and prime formation of a double stranded (ds)DNA from the single stranded DNA that makes up the viral genome (R. J. Samulski, Berns, Tan, & Muzyczka, 1982; Senapathy, Tratschin, & Carter, 1984). They also serve as an identification site for the Rep 78/68 proteins for nicking of viral dsDNA, a process necessary for replication (Im & Muzyczka, 1990). In addition to the transfer plasmid containing the viral genome, usually one or two plasmids are added containing the previously mentioned AAV proteins as well as the helper virus proteins. These viral proteins allow the producer-cells to create and package the rAAV. Following transduction of target cells by the rAAV, the single stranded DNA is turned into a double stranded viral genome by hijacking the cells replication machinery. This viral genome persists primarily in an episomal state, but integration into the host genome has been reported. The transgene or transgenes are then produced from the viral dsDNA (Hanlon et al., 2019; McCarty, Young, & Samulski, 2004; X. Sun et al., 2010).

AAV capsids for retrograde transport

As was briefly mentioned before, modifications of AAV capsid proteins in order to modify immunogenicity (Barnes, Scheideler, & Schaffer, 2019), change tropism (Girod et al., 1999; Ho et al., 2009), or add some other feature has seen a lot of interest (Viney et al., 2021). One such feature which has been of great interest to the neuroscience community is the introduction of capsids with significant amounts of retrograde transport (Davidsson et al., 2019; Tervo et al., 2016). While some wildtype (wt) AAV capsids have been found to be able to confer a certain degree of retrograde

transport to rAAVs, modified capsids have been developed which perform significantly better than wildtype capsids. Insertion of a polypeptide into the heparan sulphate proteoglycan-binding motif, followed by *in vivo* selection generated capsids capable of retrograde transport in different neurons. One of these, AAV2-Retro has seen extensive use and the first round of *in vivo* selection was performed through injection in the SNpr followed by harvesting of virus in the striatum. This and the fact that it has been used to transduce dMSN and iMSN in a different paper, made it seem like an ideal candidate to complement the LV approach (Tervo et al., 2016).

An introduction to miRNA biogenesis

MiRNA are small 20-24 nucleotide single stranded RNAs used by cells for regulation of protein expression (Ambros, 2004; Fabian, Sonenberg, & Filipowicz, 2010; Huang et al., 2011; R. C. Lee, Feinbaum, & Ambros, 1993). They are produced either by transcription of primary miRNA (pri-miRNA) from miRNA genes by RNA polymerase II (Y. Lee et al., 2004) or III (Babiarz, Ruby, Wang, Bartel, & Blelloch, 2008; Pfeffer et al., 2005). These pri-miRNA are then cut into precursor-miRNA (pre-miRNA) by the RNA nucleases DGCR8 and Drosha (J. Han, 2004). Pre-miRNAs may also be formed as part of an exon or intron (Babiarz et al., 2011). Once this pre-miRNA has been formed, it is transported out of the nucleus by Exportin 5 and further cut in the cytosol into the passenger and guide strand by Dicer. The passenger and guide strand are loaded onto Argonaute (AGO) protein which then removes the passenger and keeps the guide to act as the mature guide miRNA to form the RNA induced silencing complex (RISC) (O'Carroll & Schaefer, 2012).

Regulation through the RISC

The central component of the RISC is the AGO protein. In humans there are four different AGO proteins, 1-4, of which only AGO 2 has nucleolytic activity (Liu, 2004). If the sequence is completely complementary, the AGO2 protein is capable of cutting the targeted mRNA, causing its degradation and preventing any translation from it (Ambros, 2004; Fabian et al., 2010; Huang et al., 2011; R. C. Lee et al., 1993). For sequences that are not fully complementary, or when the miRNA is bound to one of the AGO proteins lacking nucleolytic activity, the RISC usually downregulates transcription either by sterically blocking the interaction of eukaryotic initiation factor 4E and 4G or through deadenylation of the poly-A tail (Iwasaki, Kawamata, & Tomari, 2009). For deadenylation, interaction with the protein GW-182 is required, which

helps recruit the CCR4:NOT and DCP1:DCP2 complexes, responsible for deadenylation and de-capping (Behm-Ansmant, 2006; Eulalio, Huntzinger, & Izaurralde, 2008; Rehwinkel, 2005). The RISC has also been found to locate bound mRNA to P-bodies, cellular compartments involved in mRNA storage and degradation (Hubstenberger et al., 2017; Sheth, 2003).

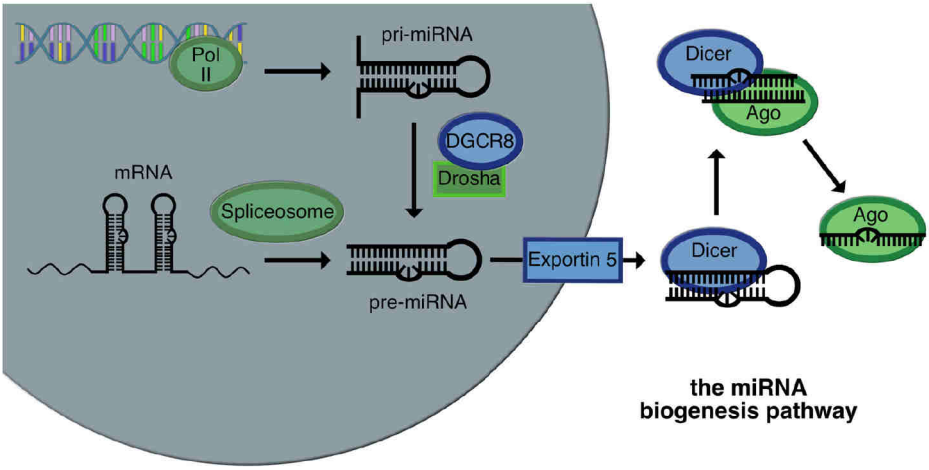

Figure 2: Illustration of the most common pathways for miRNA biogenesis.

MiRNA in brain development

Considering as much as 60% of all genes within the human genome are thought to be regulated by miRNA (Friedman, Farh, Burge, & Bartel, 2008), it is perhaps not surprising that they play an important role in brain development. Knockdown of Dicer in mice leads to death of the embryo during development (Bernstein et al., 2003), while the effect of knockdown of Dicer in neuronal cells varied somewhat, severe developmental defects of the brain, or premature death of the animal was consistently observed (Kawase-Koga, Otaegi, & Sun, 2009; McLoughlin, Fineberg, Ghosh, Tecedor, & Davidson, 2012). Targeting of Dicer in specific neuronal populations did however have more varied effects. Cuellar *et al.* looked at the effects of knocking out Dicer in D1-R cells. These mice died after roughly 74 days due to a lack of food intake causing severe weight loss from roughly 6 weeks of age. Examination of brains from 5 weeks old mice showed a reduced brain weight when compared to wt and as expected

a marked decrease in miRNA in the striatum. They had expected to see a degeneration of neurons within the striatum; however, they found no decrease in neuronal numbers compared to wt. Looking at the neuronal cell-bodies they did however find that they were 20-30% smaller in Dicer knockout mice (Cuellar et al., 2008). Similar studies have been performed in other neurons, such as dopamine neurons (J. Kim et al., 2007), Purkinje cells (Schaefer et al., 2007) and Calmodulin kinase II positive neurons (Davis et al., 2008). Dicer knockout consistently has a negative impact on the cells, leading either to abnormal morphology, behaviour, cell death, or death of the animal.

Knocking out Dicer is a major disruption of cellular function; an interesting question is whether major impact on the developmental level can also be achieved through disruption of specific miRNA. Indeed, disruption of miR-9 in mice led to live-born pups, but with severe growth retardation that died within one week. Further analysis of the brains of these mice showed reduction in size of the cerebral hemispheres and olfactory bulb (Shibata, Nakao, Kiyonari, Abe, & Aizawa, 2011; Zhao, Sun, Li, & Shi, 2009). These severe effects on brain development were seen, despite the fact that roughly 25% of the miRNA was still being expressed, further emphasizing the importance of proper expression levels. Many other miRNAs such as miR-124, let-7b, the miR-17-92 cluster, miR-137 and others have also been found to play a necessary role for proper development of the brain or specific parts of it (Akerblom et al., 2014; Akerblom et al., 2012; Bian et al., 2013; Lim et al., 2005; Rebecca Petri, Malmevik, Fasching, Åkerblom, & Jakobsson, 2014; Rajman & Schratt, 2017; Sanuki et al., 2011; G. Sun et al., 2011; Zhao et al., 2010).

MiRNA in neurodegenerative disorders

With such a significant impact on neural function, it is perhaps not surprising to find that expression levels of specific miRNAs are altered in many neurodegenerative disorders. Of course, a change in expression levels of specific miRNA does not necessitate a causative correlation, rather the changes may occur as a consequence of the cell trying to deal with the actual cause. Regardless, knowledge of differences in miRNA expression levels because of disease, can still serve a purpose for detecting proteins that might be interesting for disease progression, diagnostics, or for gene regulation.

MiRNA in PD

For the purpose of diagnostics, identification of differential expression (DE) of miRNA from blood, saliva, or Cerebrospinal fluid (CSF) in PD patients has attracted much attention. The ease with which saliva and blood especially can be extracted from a patient, has made it very desirable to detect a miRNA profile that allows for reliable diagnosis of disease. While there have been multiple different miRNAs reported to be differentially expressed between PD patients and healthy controls, very few are found across multiple different experiments. A meta-analysis looking at DE across post-mortem brain tissue, blood-derived samples, and CSF, found only 3 miRNAs of the 125 analysed, 132-3p, 497-5p, and 133b, to be differentially expressed in brain tissue. For blood derived samples, as many as 10 of 31 studied miRNA showed significant DE with miR-221-3p and 214-3p showing the most significant down-regulation. An interesting group of miRNAs are miR-29a/b/c two of which, miR-29a-3p and miR-29c-3p, were down regulated across several different studies (Bai et al., 2017; Botta-Orfila et al., 2014; Maciotta, Meregalli, & Torrente, 2013; Margis, Margis, & Rieder, 2011; Schulz et al., 2019). In a study looking at this family more closely, increasing down-regulation of in particular miR-29b was linked to decreased cognitive performance in PD patients (L. Han et al., 2020). Something that becomes clear when looking at reviews and summaries of papers published on the topic, is that many miRNAs are found to be differentially expressed in only one or two papers (Cao et al., 2017; Patil et al., 2019; Roser, Caldi Gomes, Schünemann, Maass, & Lingor, 2018). This lack of reproducibility of a clear miRNA PD profile poses a major hurdle for the establishment of miRNA profiling as a reliable and more broadly applicable tool for diagnostics.

MiRNA in HD

MiRNA DE has not been as widely studied in HD as in PD, however similarly to miRNA DE studies performed in PD, there is a lack of overlap between different studies. A recent study on miRNA levels in CSF identified 6 potential markers (E. R. Reed et al., 2018). Another study looking at miRNA levels of specific miRNAs in brain tissue yielded three different miRNA as significantly differentially expressed (Johnson et al., 2008), the findings of which were in term partially contradicted by a different study (Packer, Xing, Harper, Jones, & Davidson, 2008). More interesting is perhaps studies involving the expression of miRNAs by rAAVs in large transgenic animal models expressing mutant Huntingtin (*mHTT*). One such study, targeting exon 48 of human *mHTT* with 73 CAG repeats, expressed an artificial miRNA with which they were able to downregulate the expression of *mHTT* mRNA and protein up to 6 months post injection (Pfister et al., 2018). Another study, using a different artificial miRNA

targeting exon 1 of a 124 CAG repeat human *HTT* expressed in minipigs showed similarly encouraging results. Expression of the artificial miRNA was maintained for at least 12 months and lead to as much as 84% lowering of *mHTT* protein in the putamen and 78% in the caudate (Vallès et al., 2021). Both studies demonstrated the possibility of rAAVs to drive long-term expression of transgenes and the abilities of miRNAs to downregulate dysfunctional proteins in large animal models.

Determining DE between different miRNA populations

There are essentially two major steps involved in the determination of DE between miRNA populations of different cell-types. First the miRNA of a specific cell-type needs to be separated from that of other cell-types. This can be done through separation of the cells themselves, often through fluorescence-activated cell sorting (FACS) or affinity chromatography, or through marking of the miRNA specifically inside the cells of interest. Both FACS and affinity chromatography require dissociation of cells, a process which especially for cell-types like neurons, can be extremely stressful. This stress can lead to changes in gene expression which, depending on what is being studied, might occlude true DE (He et al., 2012; Richardson, Lannigan, & Macara, 2015; van den Brink et al., 2017). The main advantage with sorting cells, is the fact that retention of the whole cells means that miRNA and mRNA of the same cell-types can be sequenced instead of only the miRNA. Laser microdissection (LMD) similarly to FACS allows for sorting of whole cells. As implied by the name, a laser is used to cut out a marked area in a sectioned piece of tissue. The tissue within the excised area is then transferred to a well or tube for further processing (Merienne et al., 2019; Schüitze & Lahr, 1998).

Labelling of the miRNA in some way through expression of a transgene in specific cells that either label the miRNA chemically, or that bind the miRNA, allows for more immediate lysis and dissociation of cells. This prevents or reduces the impact of dissociation induced cell stress on miRNA expression. Examples of chemically altering miRNA includes mime-seq, TU-tagging of RNA, or EC-tagging. All these methods rely on the introduction of a transgene, such as Arabidopsis thaliana methyltransferase (Ath-HEN1) (Alberti et al., 2018), uracilphosphoribosyltransferase (UPRT) (Matsushima et al., 2018), or UPRT and cytosine deaminase (Hida et al., 2017), to convert or add a chemical group to the miRNA in a cell-specific manner. Cell-type specific MiRNA purification is also possible through the expression of miRNA binding proteins, fused to a tag targetable with antibodies, in a cell-type specific manner. This has been done through attachment of a GFP or Myc tag to the previously described

AGO-protein. The tag and by extension AGO-protein, along with bound miRNA can be affinity purified using antibodies targeting the tag. The miRNA can then be separated from the AGO-protein and quantified. Since only transduced cells express the tag-AGO fusion protein, only the miRNA population of these cells will be quantified. This method, known as miRNA affinity purification (miRAP) allows for isolation of desired miRNA populations and if desired, attached mRNA targets. Because of its proven history and due to the experience of other groups in our vicinity with this method, it seemed like the best choice for our purpose (He et al., 2012; R. Petri et al., 2017)

Quantification methods for small RNA

Having successfully isolated miRNA, it is necessary to quantify the specific miRNA species present in each sample. There are three commonly used methods to do this, quantitative Reverse Transcriptase PCR (RT-qPCR), microarrays, or RNA sequencing. RT-qPCR requires less starting material, has a broader dynamic range and is cheaper (depending on the number of miRNAs analysed). However, RT-qPCR requires specific primers, meaning that it is only useful for examining relative expression levels of known miRNA. As such it is generally not a suitable method for determining DE between miRNA populations of different samples where there is no prior knowledge. Instead, one needs to use one of the other two methods, microarrays or RNA-seq, both methods with their own advantages and disadvantages. With microarrays the primary advantages compared to RNA-seq are cost, smaller size of data output, reduced variation as well as more standardized analysis methods. The advantages of RNA-seq on the other hand are an increased dynamic range, improved detection of low-abundance transcripts, and a lower requirement for quantity of miRNA. For the purpose we had in mind, detection of DE between miRNAs, both abundantly and scarcely expressed, in samples containing small amounts of miRNA, RNA-seq seemed like the best choice (Giraldez et al., 2018; Mestdagh et al., 2014).

Aims of the thesis

The aim of the thesis was to determine the miRNA populations of the dMSN and iMSN of the rat striatum. We sought to target these different populations based on their projections, rather than their expression-profile and therefore used viruses capable of retrograde transport. This was to be combined with miRAP to extract miRNA from transduced cells followed by RNA-seq to attain the miRNA profile of these two neuronal populations.

For Paper I we wanted to optimize the production and transduction of a lentivirus to use for miRAP and confirm that we could transduce MSN following injection into the SNpr and GP.

For Paper II we wanted to confirm that AAV produced using a simpler protocol for production did not significantly change the virus ability to transduce cells or its toxicity.

For Paper III we wanted to apply the advancements we had made in paper I and II to determine the miRNA populations of iMSN and dMSN.

For Paper IV we wanted to investigate expression profile of the dopamine receptor D2 specific promote (D2SP) that we had used in Paper III.

Summary of results and discussion

The MSN of the indirect and direct pathways of the basal ganglia play an important role in understanding action selection in healthy animals as well as playing an important role in some major neurodegenerative disorders. Knowledge of the miRNA populations of these two neuronal populations might prove useful in expanding our understanding of their role in both healthy and diseased brains. Because of the role miRNA play in regulating a multitude of different genes under different circumstances, expression of specific miRNA might vary from cell-type to cell-type. They might either be causing the differences observed, occur as a consequence of them, or a combination of the two. Regardless of whether this differential expression is causative or correlative, it offers a possibility for identification of a cell as being either an iMSN or dMSN, regulation of transgenes through miRNA target sites, or identification of potential genes of interest that differ between the two types. Being able to determine these differences requires successful isolation of the different small RNA populations. We chose to use the miRAP method in order to do this. For us to be able to use miRAP we needed to express a GFP-AGO2 transgene in either dMSN or iMSN. We therefore targeted the two neuronal populations separately using retrograde transport. In paper I we worked on optimizing the production and use of a LV pseudotyped with the FuG-B/FuG-B2 envelope. We were able to significantly increase both the titers we were able to produce and the number of transduced cells.

As a modified AAV capsid with strong retrograde transport was published around the same time we were working on paper I, we started looking into using AAVs as a possible alternative. In paper II we compared a method for AAV production that had been developed by Negrini *et al.*, which was easier and faster than the commonly used iodixanol gradient centrifugation method. We were able to show that AAVs produced in this manner did not show any significant differences in their ability to express the transgene or in eliciting an immune response compared to AV produced with iodixanol gradient centrifugation.

Having established the functionality of the lentivirus and that we were able to easily produce smaller batches of AAV, in paper III we established that AAVs with the AAV2-Retro capsid expressing the GFP-AGO2 transgene could be used to target MSN by

injection into the GP or SNpr. We then employed both AAVs and LVs to transduce MSN with vectors expressing the GFP-AGO2 transgene. Cell specificity was achieved either through injection of retrograde transport of a virus injected in the GP or SNpr, or through use of the D2SP. Following miRAP and small RNA sequencing we were able to detect 8 miRNA that were differentially regulated between the two cell-types.

Finally, in paper IV we explored the expression pattern of the D2SP used in paper III. We found that the D2SP lead to expression of the transgene in $ChAT^+$ (Choline acetyltransferase) interneurons as well as some of the transduced DRD1 positive MSN.

Paper I

Our initial pilots of LVs pseudotyped with FuG-B1 resulted in retrograde transport of the virus and expression of the GFP-AGO2 transgene in roughly 936±317 neurons in direct pathway MSN. Judging from the literature on miRAP (He et al., 2012; Malmevik et al., 2015) and the experience of our colleagues, we had concerns that this number of neurons would be insufficient for purification of sufficient miRNA to detect DE. We therefore decided to try to optimize both viral production and transduction efficiency through changes in production protocols and our viral vector.

Exploring the impact of an immune response

During some of the initial viral injections we had seen signs of neuroinflammation, and we therefore decided to look at CD11b staining. We did not observe a significant correlation between an increased CD11b staining and a decrease in transgene expression. However, since Baekelandt *et al.* (Baekelandt, Eggermont, Michiels, Nuttin, & Debyser, 2003) had previously shown that there was an impact of removing serum, we decided to test the effects of serum removal from virus production on in vivo expression. We attempted to remove bovine serum albumin (BSA) from the viral prep either through the use of serum-free medium for the harvest, or spin columns with a molecular weight cut-off (MWCO) of 100 kDa.

In order to verify that removal of serum albumin had been successful, we ran a western blot with antibodies targeting BSA. We then analysed the blots for BSA bands and found strong bands for the virus batches produced with medium containing BSA, even when the virus-containing medium was filtered through a 100 kDa MWCO spin column (Figure 3A and B), but no staining for the virus produced without bovine serum (Figure 3A and B). BSA is capable of creating multimers that are greater in size than 100 kDa and is also known to be prone to attach to other proteins. We suspect

that both of these factors would likely have contributed to the inability of the MWCO spin columns to remove BSA from the virus prep. Regardless, when injecting the serum free batch into the SNpr of animals and counting the number of transduced cells in the striatum we were unable to detect any significant improvements in transgene expression compared to animals injected with a standard batch (Figure 3c). Furthermore, the immune response we had detected initially was hard to reproduce and was in fact never really something we had problems with later on in the project. It is possible that it was quite simply a matter of an inexperienced operator. As was mentioned before we also saw a non-significant correlation between CD11b staining and transgene levels. It is quite possible that there is indeed a very real correlation between an immune response and transgene expression levels, but that we were not able to detect it due to the population size being rather small. Due to the presence of an immune response not really having been an issue going forward, we decided to drop this line of enquiry.

Optimization of viral production

As we were unable to detect any significant improvements following removal of BSA, we instead looked at ways to increase the titer of the virus. We decided to try using a different version of the glycoprotein called FuG-B2 (Hirano et al., 2013) and combine it with transfection using polyethyleneimine (PEI) instead of Calcium Phosphate transfection. By combining these modifications to our production protocol, we were able to consistently achieve high titers with less starting material. The average titer of virus batches produced was increased to $4.6*10^9$ compared to $2.8*10^8$ when using FuG-B1 (Figure 4a). We also found that FuG-B2 was about three times as effective at transducing MSN (Figure 4B). Other researchers looking at the difference between the calcium phosphate and PEI transfection methods often report similar titers, with some reporting higher titers with calcium phosphate and some with PEI (S. E. Reed, Staley, Mayginnes, Pintel, & Tullis, 2006; Toledo, Prieto, Oramas, & Sanchez, 2009). However, something that is consistently reported is that the efficiency of calcium phosphate is extremely pH dependent (S. E. Reed et al., 2006). We ended up using PEI for all our future transductions and the initial high titers have been mostly consistently maintained.

We are unsure about what caused the observed increase in transduction efficiency. It is possible that the reduced starting material necessary to achieve the desired titers lead to a lower concentration of unwanted contaminants, or that the new glycoprotein caused an increase in transduction efficiency. Regardless, we found that the estimated number of total cells transduced, on average 3513±612, were most likely still not sufficient to allow for successful sequencing following miRAP and we therefore looked at other ways to increase the amount of transgene expressed.

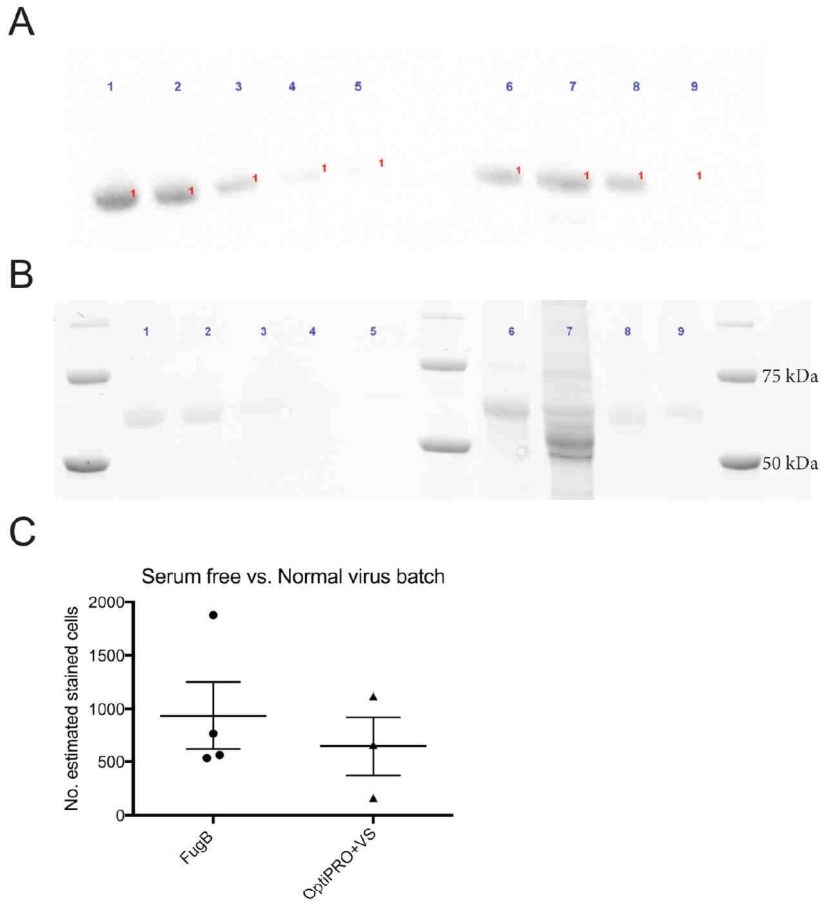

Figure 3: A) Western blot for BSA in virus batches. Lanes are loaded from left to right with 37.5, 30.0, 12.0, 6.8, 4.5 ng of BSA, a VSV-G pseudotyped lentivirus, a FuGB1 pseudotyped lentivirus pooled from a 6 times larger amount of starting material, a FuGB1 pseudotyped lentivirus pooled from a 6 times larger amount of starting material which has been concentrated and purified using a 100 kDa Molecular weight cut-off spin column, and a FuGB1 pseudotyped lentivirus made with OPTIPro serum free medium. B) Protein staining of the gel used for western blotting in A. The bands visible at roughly the same height as BSA in lanes 6–9 are most likely not BSA, but the LV envelope protein which is of almost identical size. C) The number of cells stained for GFP in animals injected with a virus batch prepared using the "standard" protocol for FuGB1 pseudotyped lentivirus or using the modified version of the protocol using OptiPRO and a Vivaspin column. There is no significant difference between the two protocols.

Improving viral expression

We next considered the possibility that not all cells that had been transduced might express the transgene in sufficient quantity to be detected. The CMV promoter that we had been using was replaced with one that is specific to neurons, the human Synapsin promoter (hSyn) (Kugler, Kilic, & Bahr, 2003; Yaguchi et al., 2013). Following this

change in promoter we observed an approximately 4-fold increase in the number of neurons expressing GFP-AGO2 compared to the CMV promoter element, with the number of transduced cells increasing from 1023±210 with the CMV promoter to 4138±1094 with the hSyn promoter element. The increase was not as large when using the GFP transgene, with a twofold increase from 6507±925 compared to 3047±976 cells (Figure 4C). The fact that the hSyn promoter led to higher transgene expression in neurons was supported by previous studies (Kugler et al., 2003; Yaguchi et al., 2013).

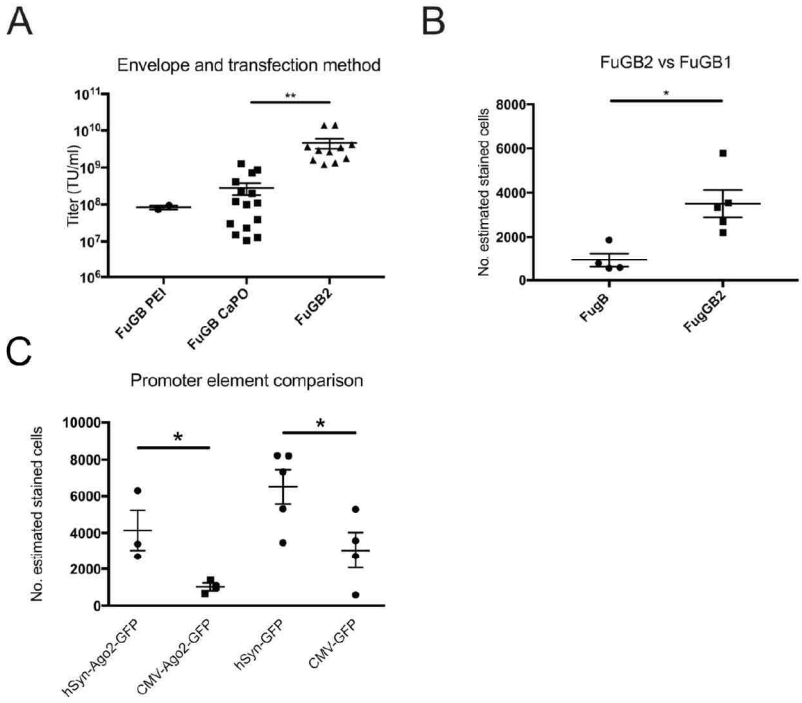

Figure 4: A) A comparison of the titer of several different batches of FuGB1 or FuGB2 pseudotyped lentivirus, using PEI or calcium phosphate as transfection agent. The titer was significantly increased, $4.6*10^9$ TU/ml compared to $2.8*10^8$ TU/ml, when using the FuGB2 envelope for pseudotyping. B) Counting the number of transduced cells using a FuGB1 or FuGB2 pseudotyped lentivirus of the same titer ($4-5*10^8$ TU/ml) showed an increase in cells from 935 ± 317.5 transduced cells, to 3513 ± 612.9 transduced cells. C) A comparison of the CMV and hSyn promoter showed increase numbers of transduced cells with hSyn.

Testing injections in the GP

Having confirmed the transduction of some 6000 neurons following injection of the LV in the SNpr, we proceeded to test if we could achieve similar results when we performed injections in the GP. Because the GP is adjacent to the striatum, we ensured

that we could observe retrograde transport by counting the number of cells that were stained for GFP and DARP32, a marker of MSN, close to the injection site or further away. Our reasoning being that local diffusion of the virus would transduce cells roughly 1 mm away from the injection site (de Almeida, Zala, Aebischer, & Deglon, 2001), while retrograde transport would lead to transductions of neurons further away. We also expected to see only MSN transduced further away, since the interneurons only make within the striatum. Indeed, this was also what we observed with almost no non-MSN cells transduced in sections 2.4-2.8 mm from the injection site compared to around 2% roughly 0.6 mm away (Figure 5).

Testing miRAP

Having increased the number of transduced cells roughly 6-fold, we performed injection of virus in the SNpr and performed miRAP to purify miRNA using striatal tissue. We then performed RT-qPCR with four sets of primers targeting miR-103-3p, an endogenous control (Finnerty et al., 2010), miR-124-3p, a neuronally expressed miRNA(Jovicic et al., 2013; Malmevik et al., 2015), miR-21a-3p, an astrocyte specific

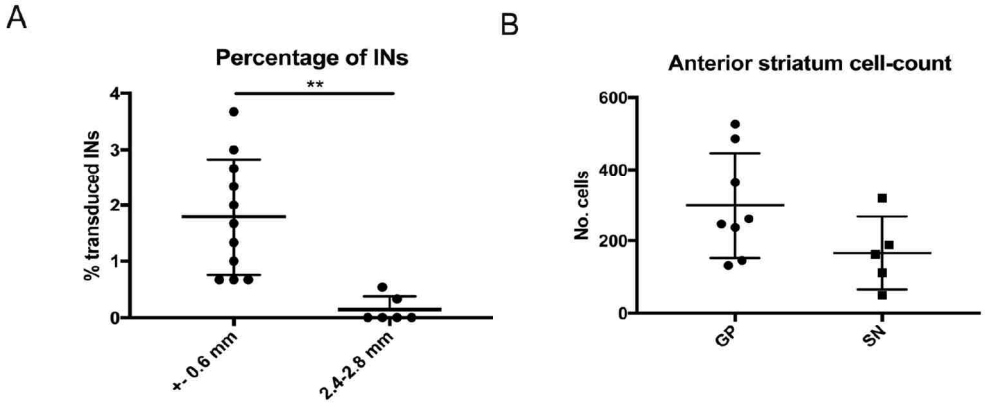

Figure 5: A) The number of GFP$^+$/DARP32$^-$ cells were counted either within diffusion distance of the virus from the injection site in the GP or further away in the striatum. The relative lack of GFP$^+$/DARP32$^-$ cells further away indicate successful retrograde transport of the virus. B) The number of transduced cells in the anterior part of the dorsal striatum were compared following injection into GP or SN.

miRNA (Jovicic et al., 2013) and the U6 spike-in. While the amount of miRNA in the samples affinity purified with a GFP antibody was up significantly compared to controls using a Vmat2 antibody or the left hemisphere striatal section (Table 1), miR-21a-3p was not present in sufficient quantities in most samples to be detected. Because

of this we were unable to tell if there was any enrichment of neuronal miRNA in our miRAP samples compared to miRNA purified from the total tissue.

In summary, with Paper I we showed that we were able to successfully transduce cells using a FuG-B2 pseudotyped lentivirus and perform miRAP in order to purify miRNA from transduced cells. We also optimized production methods and vector design to increase the number of neurons we were able to transduce. Furthermore, we showed that the LV could be used to transduce both dMSN and iMSN.

Table 1: RT-qPCR using primers targeting miR-124, miR-103, and U6 spike in controls. Neg ctrl and AB ctrl both had much lower Cp-values of miR-124 and miR-103 indicating successful miRAP.

	1	2	Neg ctrl	AB ctrl	1 tot	2 tot	Neg ctrl tot	AB ctrl tot
U6	22.53	21.27	20.73	20.12	19.99	19.95	19.92	19.66
103	27.41	25.77	31.11	29.74	21.30	22.05	22.88	23.67
124	24.24	22.84	28.06	27.46	17.94	19.27	20.28	21.69
124 normalized to 103	24.24	24.48	24.37	25.13	24.06	24.62	24.81	25.43

Paper II

Because of the publication of a modified AAV2 capsid with high degrees of retrograde transport, we were interested in testing whether we could transduce a larger number of cells using AAVs. However, the commonly used method for AAV production, iodixanol purification (Iod), produces large quantities of virus (commonly between 100-200 µl) which is not optimal when performing small pilots. Fortunately for us, our colleagues (Negrini, Wang, Heuer, Bjorklund, & Davidsson, 2020) had established a protocol (Chl) that allowed for production of smaller batches (25-50 µl) of high titer AAV. In order to ensure the viability of virus produced by this method, we looked at several parameters compared to virus produced using iodixanol purification.

Viral batch protein analysis

By denaturing virus produced either through the Iod or Chl method and running it on an SDS-PAGE gel and staining for proteins, we were able to detect that the Chl method led to greater presence of BSA in the virus batch (Figure6A). To verify that there were no major changes in the capsid produced we performed western blot with antibody targeting the VP1, VP2 and VP3 protein. The three different proteins were present regardless of production method in roughly the same amounts (Figure 6B). In order to count the number of empty and loaded capsid particles, transmission electron microscopy was used, with no significant differences present (Figure 6C and D).

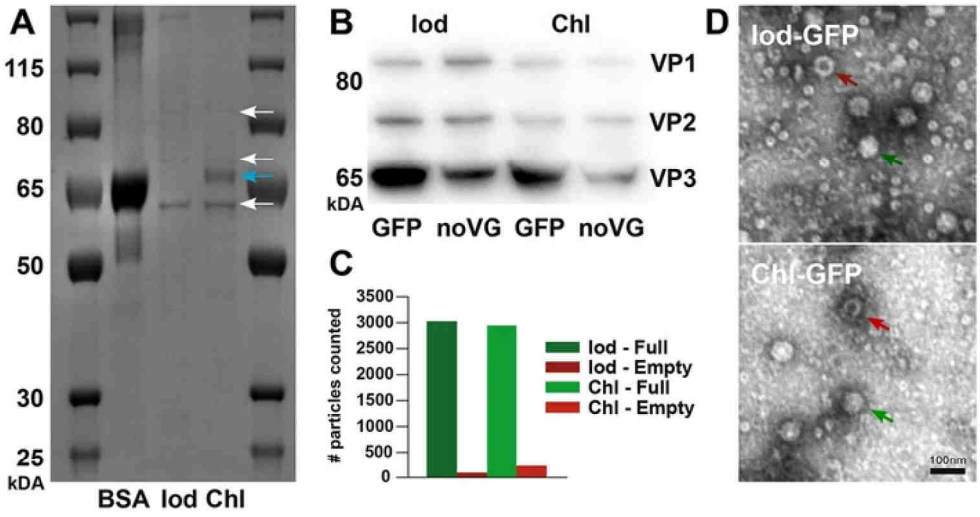

Figure 6: A) AAV batch produced either through the Chl or Iod production method was stained using Coomassie Brilliant Blue. A stronger BSA band (blue arrow) was visible in the batch produced using Chl production method. B) WB for VP1/2/3 showed similar relative amounts of the different capsid proteins between the two different production methods. C and D) Quantification of full and empty particles using TEM showed >90% full particles in both methods.

Testing transduction efficiency in vitro and in vivo

We first tested the two different virus production methods through transduction of cells *in vitro* (Figure 7). GFP expression levels were almost identical when comparing the two different production methods across a number of different titers. In order to

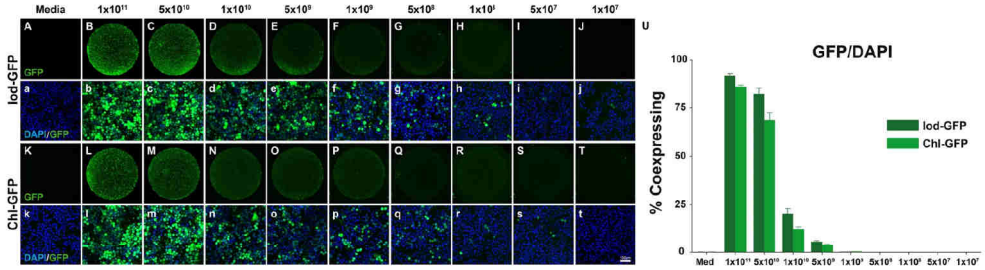

Figure 7: GFP expression in HeLa cells at different dilutions showed similar expression levels between both production methods.

test the virus *in vivo* injections were performed in the SNpc and brains stained for GFP. Once again, we were unable to detect significant differences in expression of GFP between the two production methods (Figure 8A-J).

Controlling for differences in immunogenicity

Another key factor when comparing two different viral production methods is their ability to elicit an immune response. The impact of viral production method on virus immunogenicity was therefore controlled in two different ways. First, animals were injected with virus unilaterally in the SNpc and rotations measured following amphetamine injections. Because unilateral lesions of the SNpc cause animals to rotate preferentially in the direction ipsilateral to their lesion, if one method of virus production caused large amounts of cell-death in the SNpc, we would have expected to see a preferential amount of rotation in one direction (Björklund & Dunnett, 2019). No differences were observed between virus production methods (Figure 8K). However, the observation of preferential rotation requires significant cell-death. Toxicity that might still be significant and measurable on a cellular level might occur even if there are not noticeable changes in behaviour. Sections were therefore stained for tyrosine hydroxylase (TH), a marker for dopaminergic cells in the SNpc. Both the number of TH positive cells in the SNpc and the striatal innervation of TH positive fibres in the injected compared to the un-injected side was equal across the two different production methods (Figure 8L-q).

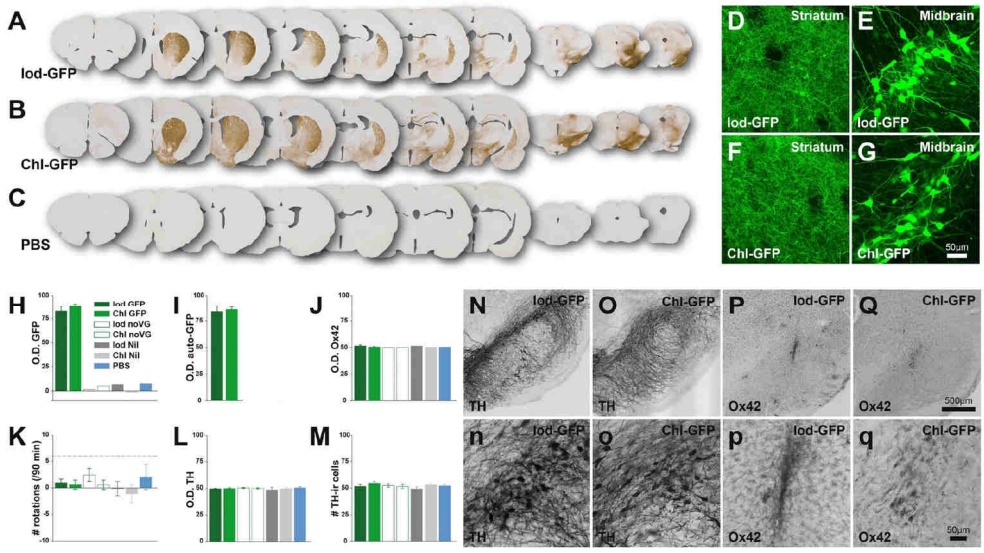

Figure 8: The two production methods were compared in vivo to test both differences in expression of a transgene and immunogenicity. Virus batches produced without transfer plasmids, without capsid plasmids and with a transfer plasmid expressing GFP was injected unilaterally into the SNpc. A-H, I) GFP expression following injection is compared between different virus batches. GFP expression was only detected in virus produced using both GFP transfer plasmid and capsid plasmid. There was no significant difference between the two production methods. K) Amphetamine rotations were used to check for significant degeneration of the SNpc. J, P-q) Ox42 staining was used to check for an increase in local microglia with no significant difference between the two production methods.

In summary, with Paper II we showed that virus produced with this chloroform purification method was just as efficient at transducing cells as virus produced with the standard iodixanol protocol. In addition, there were no measurable negative impacts on its toxicity or ability to trigger an immune response upon injection.

Paper III

Having shown that we could successfully transduce dMSN and iMSN using LVs pseudotyped with FuG-B2 and that we could produce AAVs through a less time-consuming method, we employed both these methods to perform miRAP on dMSN and iMSN.

Expanding lentiviral transduction with the D2SP

Because the dMSN send collaterals onto the GP, we were concerned that injection into the GP might transduce dMSN as well as iMSN. Fortunately, a promoter that had been shown to be highly specific to DRD2 expressing MSN had recently been published and so we decided to try it (Zalocusky et al., 2016). We observed successful expression of both a fluorophore as well as GFP-AGO2 under regulation of the D2SP following viral injection into the striatum (Figure 9).

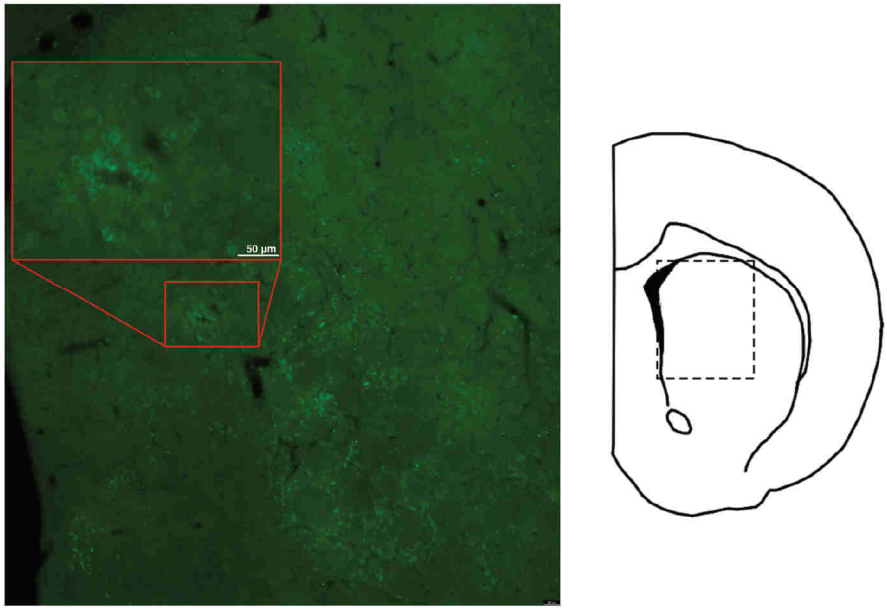

Figure 9: GFP staining of brains injected with a LV expressing GFP-AGO2 under control of the D2SP promoter showed successful transduction and expression. Localization of the imaged area was marked on a sketch.

Employing AAV2-Retro for retrograde transport of Cre

To complement our strategy of using LVs for retrograde transport, we also tested using AAVs with the AAV2-Retro capsid, to transport Cre to the dMSN or iMSN and injected an AAV with a floxed GFP-AGO2 locally in the striatum. While we did not see the numbers of transduced cells we had hoped for, it was still sufficient to perform miRAP based on transduction numbers following LV injection (Figure 10).

MiRAP on iMSN and dMSN

Having transduced iMSN and dMSN using both retrograde transport of LVs and AAVs, as well as what we thought would be iMSN with the D2SP, we performed miRAP to purify miRNA. Sequencing of the miRNA showed very large differences between the miRNA population of the neurons transduced with the D2SP regulated GFP-AGO2 virus and the miRNA populations of the neurons transduced through retrograde transport (Figure 10A). Based on the fact that the differences were so large, compared to what we saw when comparing the miRNA populations of neurons transduced through retrograde transport, we concluded that the D2SP also allowed for expression in interneurons. We therefore chose to just compare neurons transduced following injection in the GP to neurons transduced following injection in the SNpr. This comparison gave a total of 8 miRNA that were differentially expressed (Figure 10B), although none more than 6-fold. Of these miRNAs only one was detected as differentially expressed in a similar comparison (Table 2)(Merienne et al., 2019).

In summary, in paper III we combined progress made in paper I and II and implemented developments made by other groups in order to be able to perform miRNA purification. Based on these results we were able to discover DE of 8 miRNA, one of which was also discovered by another group performing a similar experiment.

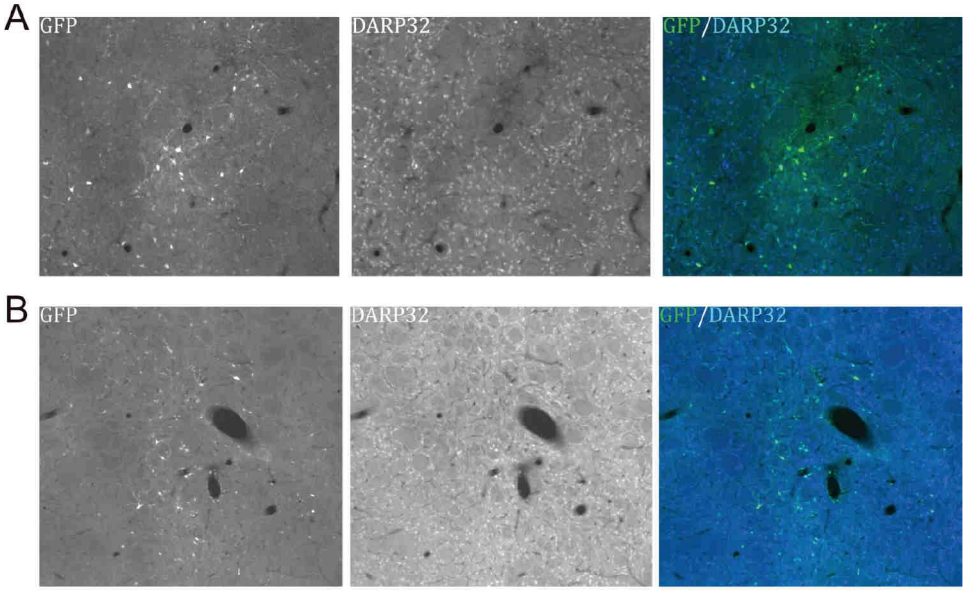

Figure 10: Expression of GFP in animals injected with AAV-Retro expressing Cre in GP (A) or SN (B). GFP and DARP32 was labelled with antibodies and counted to check whether co-labelling was lower or higher than expected through diffusion.

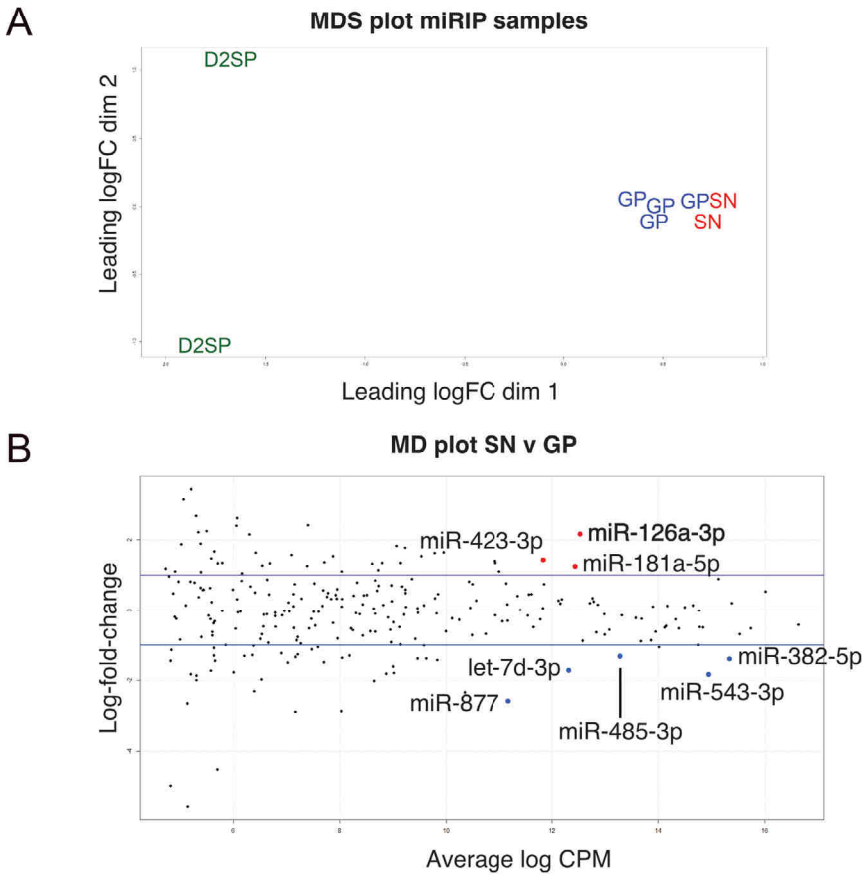

Figure 11: A) MDS plot comparing the miRNA expression of 8 different samples. As can be seen the D2SP samples were very different from the GP and SN samples. B) MD plot showing DE of miRNA between the dMSN (SN) and iMSN (GP) with the 8 miRNA found to be differentially expressed between the two populations.

Table 2: Table showing the log fold change, log counts/million, p-value and false discovery rate for the 8 miRNA found to be differentially expressed in SN compared to GP.

miRNA	LogFC	LogCPM	P-value	FDR
rno-miR-543-3p	-1.83	14.94	1.86e-05	0.0048
rno-miR-126a-3p	2.17	12.53	1.14e-03	0.0868
rno-miR-382-5p	-1.39	15.34	1.26e-03	0.0868
rno-let-7d-3p	-1.71	12.31	1.61e-03	0.0868
rno-miR-877	-2.57	11.16	1.89e-03	0.0868
rno-miR-485-3p	-1.32	13.28	2.21e-03	0.0868
rno-miR-181a-5p	1.24	12.45	2.40e-03	0.0868
rno-miR-423-3p	1.43	11.84	2.68e-03	0.0868

Paper IV

In the original paper the expression of a transgene regulated by D2SP was investigated in the Nac. They had found minimal expression in cells positive for ChAT, a known marker of a type of interneuron that also expresses DRD2. Since the ChAT positive interneurons are also found in the dorsal striatum, and because of the results of the miRNA sequencing performed in Paper III, we wanted to investigate whether the D2SP would express exclusively in MSN or also in ChAT interneurons in the dorsal striatum.

Expression in ChAT interneurons

To investigate the expression profile, we injected an AAV2/5 expressing mCherry under control of the D2SP. The number of cells that were positive for ChAT, mCherry or both were then counted to determine how specific the promoter was to MSN. We found that 91% of ChAT interneurons in the area of injection expressed the transgene, indicating that the promoter is not specific to MSN (Figure 12).

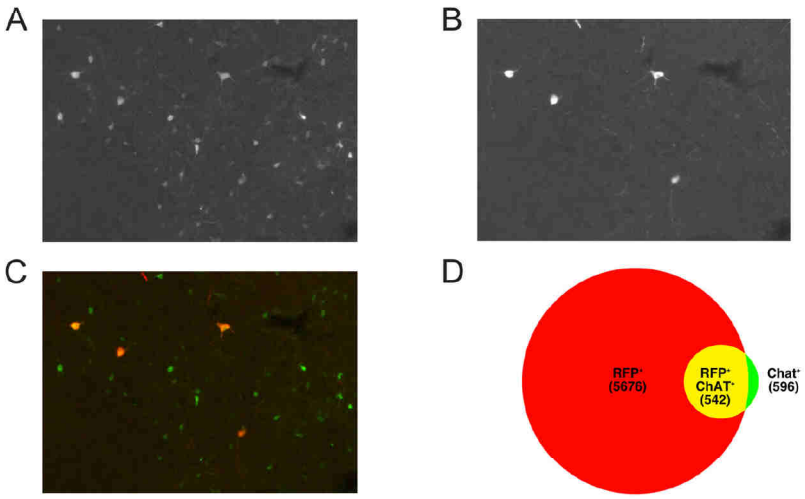

Figure 12: Staining of mCherry (A) and ChAT (B) following injection of an AAV5 expressing mCherry, under the regulation of the D2SP, in the striatum. C) Merger of A and B with ChAT in red and mCherry in green. D) Venn diagram illustrating the number of mCherry+/ChAT- cells, mCherry+/ChAT+cells, as well as ChAT+/mCherry- cells that were within the area of viral injection

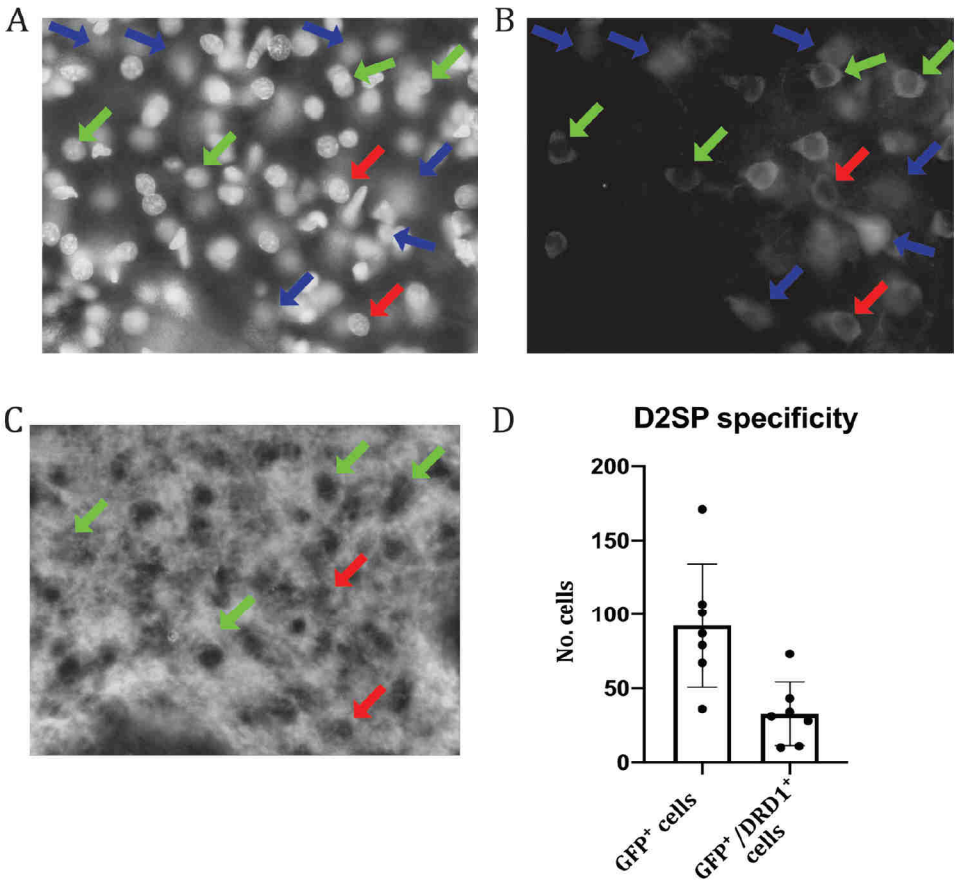

Figure 13: A-C) Images showing an example of the DAPI (A), GFP (B), and DRD1 (C) staining following injection with a LV expressing GFP-AGO2 under regulation of the D2SP. D) Quantification of the number of GFP^+ cells that were also found to be $DRD1^+$.

Specificity to DRD2 positive neurons

We then investigated the ability of the D2SP to limit expression to DRD2 positive MSN only. By staining for DRD1 positive cells and GFP (Figure 13A-C), we found that roughly 75% of all cells expressing GFP were DRD1 negative. This still leaves 25% of cells which are DRD1 positive (Figure 13D). The discrepancy between our results and previously published ones has a number of possible explanations. First the method by which we have determined whether a cell is DRD1 positive or not is not optimal with a lot of room for subjective interpretation. It is also possible that a cell is both DRD1 and DRD2 positive, something we have not controlled for. Another

explanation could be differences in expression between the MSN of the Nac and the dorsal striatum.

In summary, in Paper IV we show that the D2SP does not express exclusively in DRD2 positive MSN, but also in ChAT interneurons. Furthermore, expression also seems to occur in DRD1 positive MSN, which although not contradictory to previous results, might prove problematic if the aim is to target exclusively the indirect pathway.

In order to more accurately determine the specificity of the D2SP in regard to expression within DRD1 or DRD2 MSN exclusively, we injected a LV expressing GFP-AGO2 under control of D2SP into the striatum of rats (n=2). We used RNAscope, an *in situ* hybridization method, to determine specificity by making use of probes targeting Adora2a, DRD1 and EGFP (Figure 14A-D) to count whether cells were $GFP^+/DRD1^+$ or $GFP^+/Adora2a^+$. To our surprise we found almost no specificity towards $Adora2a^+$ cells at all, with no significant difference between the number of $GFP^+/DRD1^+$ and $GFP^+/Adora2a^+$ cells (Figure 14E). None of the GFP^+ cells we looked at were $Adora2a^+/DRD1^+$.

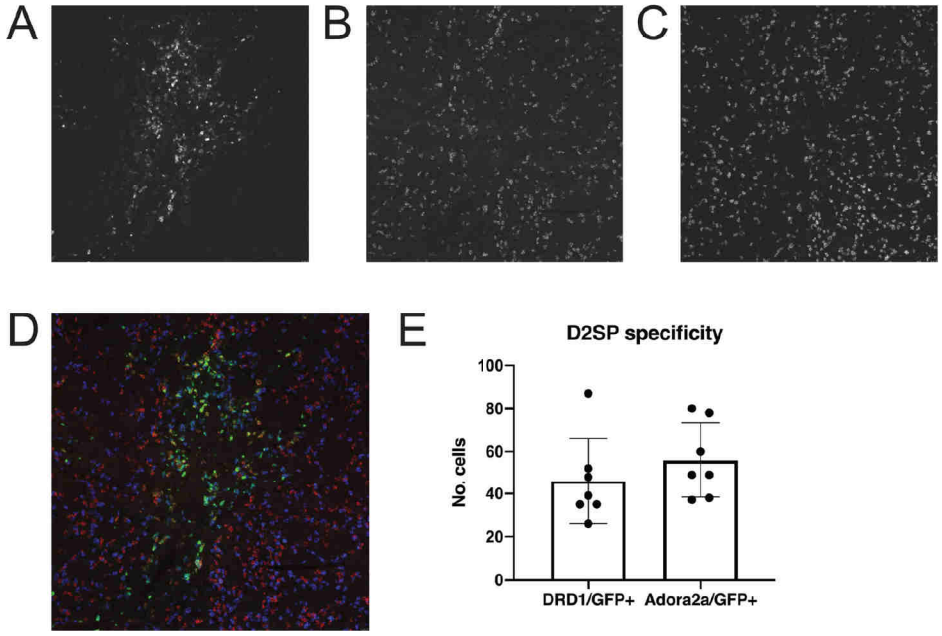

Figure 14: A-C) Images showing an example of the RNAscope staining using probes targeting GFP (A), Adora2a (B), and DRD1 (C) as well as a composite of all three with GFP in green, Adora2a in red, and DRD1 in blue (D). E) GFP+ cells were counted and then checked for colocalization with either DRD1 or Adora2a. No significant difference was observed in terms of expression level between DRD1+ and Adora2a+ cells.

Conclusion and future perspective

The expression of specific miRNAs can play an important role in regulating protein expression both in cell differentiation, normal cell states, and in diseased cell states. Knowledge of differential expression between different neuronal populations can therefore be exploited to direct expression of transgenes to specific cell types, for diagnostics, or to generate leads on potential proteins of interest in disease states or for development. Despite their important role in regulation, there is not an abundance of data concerning miRNA expression in different neuronal populations. We sought to remedy this lack of knowledge, specifically for the dMSN and iMSN.

In our pursuit of this goal, we were able to improve upon our previous production methods and improve transgene expression levels within MSN in Paper I. While we only made use of FuG-B2 pseudotyped lentivirus for expression of GFP or GFP-AGO2 in MSN, any transgene that fits into a LV could theoretically be expressed in specific MSN using this method. Obvious examples that come to mind are of course DREADDs or Channelrhodopsins useful for studying the impact of activation or inhibition, of specific neuronal populations, on behaviour. The main disadvantage, at least in most cases, of using FuG-B2 pseudotyped LVs compared to a local injection of LVs or AAVs was the lower number of cells transduced. Of course, depending on the application, a lower number of cells as well as the relatively even distribution of transduced cells throughout the striatum might be considered an advantage.

Regardless of our improvements, we were unable to achieve the number of transduced neurons we had hoped for and so looked at other candidates for achieving retrograde transport with a viral vector. AAVs are generally able to achieve both a larger spread within the brain, as well as transducing a larger number of neurons in comparison to LVs due to the increased number of viral particles. We therefore tried producing and injecting AAVs with a capsid engineered for retrograde transport. In Paper II we tested a newly developed AAV production method to see how well it compared to the standard method. We found no significant differences in composition of the virus or toxicity when comparing the two methods. This new production method allowed us to easily produce multiple different batches to test out different constructs and capsids. While not generating data included in this thesis, it did allow us to probe many different

approaches to achieve our goals that would otherwise have been costly and time-consuming with the standard method.

With the methods outlined in Paper I and II, in Paper III we were able to perform miRAP to sequence the miRNA population of MSNs. We had hoped to be able to find greater numbers of more strongly DE miRNA to use for miRNA dependent transgene regulation. We had also hoped that the D2SP would be specific and would provide us with an iMSN specific miRNA population, however when we analysed the miRNA sequencing data, we found that this was most likely not the case. Indeed, as would later be shown in paper IV, the D2SP was more than capable of high levels of expression in ChAT+ interneurons. However, we nonetheless decided to continue with the data that we did have from retrograde transport following injections into the GP or SNpr. We were able to find eight miRNA that were DE between what we thought was a population of dMSN miRNA and a mix of dMSN and iMSN miRNA. Of the miRNA that we did find to be differentially expressed in Paper III, miR-126a-3p was the most interesting as it had also been identified by another group looking at miRNA DE between iMSN and dMSN (Merienne et al., 2019). TargetScan (Agarwal, Bell, Nam, & Bartel, 2015), a tool for predicting miRNA targets within protein UTR's, suggested a total of 20 predicted targets, of which Protein kinase C (PRKCA) (Fieblinger et al., 2014), Regulator of G-protein signalling 3 (RGS3) (Burchett, Bannon, & Granneman, 2001), Polo-like kinase 2 (PLK2) (Dzamko, Zhou, Huang, & Halliday, 2014), and A-kinase anchor protein 13 (AKAP13) (Poelmans, Franke, Pauls, Glennon, & Buitelaar, 2013) are involved in signalling pathways. In addition, Sprouty-related, EVH-1 domain-containing protein 1 (SPRED1) (W. Kim et al., 2014), EF-hand domain family, member D2 (EFHD2) (Borger, Herrmann, Mann, Spires-Jones, & Gunn-Moore, 2014), Protocadherin 7 (PCDH7) (Pancho, Aerts, Mitsogiannis, & Seuntjens, 2020), Calmodulin-regulated spectrin-associated protein 1 (Camsap) (Leterrier, 2018), and Plexin-B2 (PLXNB2) (Simonetti et al., 2019) are involved in synapse modulation and axon growth.

It is enticing to speculate what role might be played in MSN by these proteins and whether they are expressed or not. RGS3 for example has been shown to be present in dMSN, to be regulated by DRD1 activation (Burchett et al., 2001), and to inhibit activation by Gq through hydrolysis of bound GTP (Scheschonka et al., 2000). Similarly, Plk2 also acts to inhibit an increase in excitability of the neuron, by downregulating the amount of AMPARs that are incorporated into the membrane (Kea J. Lee et al., 2011; Zhu, Qin, Zhao, Van Aelst, & Malinow, 2002). On the other hand, PRKCA activation seems to lead to increased excitability in hippocampal neurons and is necessary for LTP (Colgan et al., 2018), but seems to fill an opposing function in cerebellar purkinje cells (Leitges, Kovac, Plomann, & Linden, 2004).

Targeted downregulation of these miRNA is a potential future avenue of exploration. This could be done either through the introduction of virus expressing miRNA sponges, knockdowns, or transgenic animals. Such experiments would hopefully improve our understanding of the role played by these miRNAs and their targets. Another interesting topic to explore would be differences in disease models such as 6-hydroxydopamine (6-OHDA), LID models, or HD models, both for differences in overall miRNA population, but also to analyse differences specific to dMSN or iMSN as it might help expand our knowledge of cellular changes in these models. Changes such as those seen in the dMSN following dopamine denervation and LID (Fieblinger et al., 2014; Sebastianutto et al., 2020).

We had hoped that we would be able to find DE of miRNA between iMSN and dMSN large enough to support miRNA regulated inhibition of transgene expression, as has previously been done in the brain using miRAP data from GABAergic interneurons of the cortex. A vector targeting inhibitory interneurons in the cortex with a high degree of specificity was constructed using target sites for miR-128 and miR-221, which was expressed 16 and 12-fold higher in excitatory neurons in the cortex (Keaveney et al., 2018; Sayeg et al., 2015). Unfortunately, the differences we detected were much smaller than that and so we did not think it likely to be able to successfully construct a vector capable of expression in one population over the other while still maintaining acceptable expression levels.

Materials and Methods

For the materials and methods section, we have chosen to focus primarily on the work present in the first author papers and manuscripts that were primarily carried out by the author.

Animal work

All animals were housed and handled in accordance with the principles of "Guide to the Care and Use of Experimental Animals". All procedures have been approved and performed according to the guidelines established by the Ethical Committee for Use of Laboratory Animals at Lund University under the permit M24-15 or M18184/17 for paper I, III and IV. 77 female Sprague dawley rats (Charles River, Sulzfeld, Germany) weighing 225-250 g were used for the experiments performed in paper I, III and IV. 53 female Sprague dawley (Janvier) rats were used in paper II. In total 128 animals were used for the experiments.

Stereotactic surgery

Rats were anaesthetized by injecting fentanyl (1.56 ml/animal, 50 g/ml fentanyl, B. Braun) and medetomidine (0.14 ml/animal, 1 mg/ml Domitor, Orion Pharma Animal Health) intraperitoneally (i.p.) in papers I, III and IV. After the pain reflex in the hindlimb was gone, the scalp was shaved, and the rat was mounted in the frame using ear- and a tooth-bar. For papers III and IV, Bupivacaine (0.1 ml/animal, 1 mg/ml, Marcaine, Astra Zeneca) was injected and spread across the scalp. The skull was laid bare using a scalpel and the bregma was located and set as point zero for all axes. Lambda was used to determine that the head was flat. The skull bone covering the intended injection site was drilled away until only a thin layer remained which was punctured and carefully removed using a very fine tweezer. At the intended injection site, the intact dura mater was then punctured using a sterile syringe needle. The capillary was gently inserted and moved down 1 mm into the brain to ensure entry without a need to push the brain down. The capillary was then cleaned using 3% H2O2 and H2O upon which the virus was loaded. After retraction of the capillary, it was

cleaned using H2O2 and H2O before being used for the next injection. After injections were finished, the skin was sealed with a suture, the rat was then marked in the ear and was taken out of anaesthesia by i.p. injection of atipamezolhydroklorid (0.013 ml/animal, 5 mg/ml, Antisedan, Orion Pharma Animal Health) and in paper I, buprenorphine (0.03 ml/animal, 0.3 mg/ml, Temgesic, Indivior).

Table 3: Injection coordinates for the different viral injections. Paper in which coordinates were used are listen in brackets.

Injectionsite	A/P	M/L	D/V	Viral volume
LV SNpr (I)	-5.4	1.5/2.5	-7.8/-7.4	1 µl+1 µl
LV GP (I)	-0.8	3.5	-6.1	1 µl
LV SNpr (III)	-5.3	1.8/2.6	-7.8/-7.4	1 µl+1 µl
LV GP (III)	-0.8	-3.0	-6.1	1 µl
LV Striatum (III, IV)	0.7	-3.0	-3.5/-5	1.5 µl+1.5 µl
AAV SNpr (III)	-5.2	1.8/2.6	-8.2/-7.8	1 µl+1 µl
AAV GP (III)	-0.8	-3.0	-6.1	0.5 µl
AAV Striatum (IV)	0.7	-3.0	-3.5/-5	1.5 µl + 1.5 µl

Perfusion and tissue sample collection

For IHC and RNAscope rats were sacrificed by i.p. injection of sodium pentobarbital (1.5 ml/animal, 60 mg/ml, Apl). Brains were fixed using 4% PFA pumped into the vascular system of the upper body. After the initial fixation, the brain was removed from the skull and incubated in 4% PFA for another 2-24 hours at 4°C. The brains were then moved to 15% or 25% sucrose solution (For RNAscope and IHC respectively) and incubated at 4°C for 24-48 hours, until the brains would sink to the bottom of the flask.

For miRAP fresh striatal tissue was collected. Rats were sacrificed by i.p. injection of sodium pentobarbital (1.5 ml/animal, 60 mg/ml, Apl). Following loss of the pain reflex animals were decapitated and brains removed from the skull and washed using ice-cold saline-solution. The brain was then placed inside a mould containing cut-outs for double-edge razor blades 1mm apart allowing for coronal sections. A razorblade was inserted 5 mm from the anterior of the brain, excluding the olfactory bulb, cutting the brain along the coronal plane. A second blade was inserted 7 mm from the anterior of the brain, excluding the olfactory bulb, cutting the brain a second time along the coronal plane. The 2 mm thick piece was then move to a glass plate with saline solution that was kept on ice. The right and left striatum were cut out with the bottom part, below the anterior commissure being removed.

Immunohistochemistry

In order to section the brain, it was placed on a microtome using cryo-mounting medium and frozen using dry-ice. The brain was then cut into 35 µm thick sections. Every 6th section belonged to the same series. Brain sections were stored at -20°C in wells of a 12-well plate containing antifreeze.

Each series to be stained was washed three times in KPBS. After washing, sections were incubated in 1 ml of quenching solution for 15 minutes. Sections were then washed in KPBS 3 times. This step was followed by a 1 hour Incubation of the sections in 1 ml 5% serum solution. The sections were then incubated in 1 ml primary Ab diluted in 5% serum over night at RT or 4°C over the weekend.

Following incubation, the samples were washed twice with KPBS. The sections were then incubated in 5% serum solution for at least 15 minutes, followed by a 1 hour incubation in 1ml secondary AB diluted in 5% serum.

Following the 1 hour incubation in secondary AB, the sections were washed in KPBS three times. If secondary antibodies conjugated to a fluorophore had been used, the sections were mounted or stored at 4°C until mounting. If a secondary conjugated to biotin was used, the sections were incubated in 1ml ABC complex for 1 hour and then washed with KPBS 3 times.

1 ml of DAB solution was added to the sections and incubated for 2 minutes. This was followed by a 10 µl addition of H_2O_2 solution and incubation until colour developed, but a maximum of 4 minutes. All the sections that were to be compared were incubated for the same amount of time.

The sections were then washed twice in KPBS. After washing, the sections were mounted on microscope slides and left to dry. Having dried, the slides were incubated in H2O and if secondary antibodies conjugated to fluorophores were used, coverslipped using PVA-DABCO with or without DAPI at a 1:1000 dilution. If secondary antibodies conjugated to biotin was used, incubation was continued using ethanol and finally xylene to dehydrate. All incubations were carried out for 2 minutes. DPX was then used as a mounting medium and the slides were coverslipped.

Serum solution was prepared using blood serum of the species used to produce the secondary antibody.

Table 4: List of all the antibodies, both primary and secondary used in the papers.

Species	Antigen	Dilution	Conjugate	Cat. No., company
Mouse	Rat CD11b	1:1000	N/A	MCA275, G Serotec
Rabbit	GFP	1:5000	N/A	Ab290, abcam
Chicken	GFP	1:1000	N/A	Ab13970, abcam
Rabbit	DARP-32	1:1000	N/A	AB10518, Millipore
Mouse	GFP	1:1000	N/A	Ab1218, abcam
Chicken	mCherry	1:1000	N/A	Ab205402, Abcam
Goat	ChAT	1:500	N/A	AB144P, Merck-Millipore
Rat	DRD1	1:10000	N/A	D2944, Sigma-Aldrich
Rabbit	DRD2	1:500	N/A	AB5084P, Merck-Millipore
Mouse	Enkephalin	1:250	N/A	AB150346, Abcam
Goat	Chicken-IgY	1:500	Alexa 488	A11039, Thermo Fisher
Goat	Rabbit-IgG	1:500	Alexa 555	A27039, Thermo Fisher
Goat	Rabbit-IgG	1:800	Alexa 405	A31556, Thermo Fisher
Goat	Rabbit-IgG	1:800	Alexa 488	A-11008, Thermo Fisher
Donkey	Goat-IgG	1:400	Cy3	705-165-003, Jackson Immuno
Goat	Mouse IgG	1:500	Alexa 555	A28180, Thermo Fisher
Goat	Rat IgG	1:800	Alexa 555	800A-21434, Thermo Fisher
Goat	Rabbit-IgG	1:200	Biotin	BA 1000, Vector Labs

RNAscope

RNAscope was performed following the protocol for fixed frozen tissue. Rats were sacrificed and perfused as described previously. Following fixation and incubation in sucrose, the brains were frozen using crushed dry-ice and stored at -80°C until cut. Before cutting frozen brains were incubated at -20°C for 1 hour. Brains were then sectioned in 10um thick sections using a cryostat at -20°C. Brain sections were captured using SuperFrost Plus slides, 1 section per slide. They were then stored at -20C for 1-2 hours to dry. Sections were then post-fixed through incubation in 4% PFA for 15 minutes at 4°C, followed by dehydration through incubation in gradually increasing concentrations of ethanol at RT for 5 minutes (50%, 70%, 100% x2). Finally, the slides were dried at RT for 5 minutes.

Five drops of RNAscope Hydrogen peroxide were then applied to the sections and incubated at RT for 10 minutes. Hydrogen peroxide was then removed, and sections washed in distilled water. The sections were then placed in a rack in boiling (95+°C) target retrieval reagent for 5 minutes and then immediately washed in distilled water followed by a wash in 100% ethanol. Slides were dried at RT and a hydrophobic barrier was applied around the section. 5 drops of Protease were then applied to each section followed by a 30-minute incubation at 40°C in a humidity-controlled oven. Sections were washed using distilled water.

Following the wash, probes targeting Adora2a (Biotechne, cat no: 450471), DRD1 (Biotechne, cat no: 317031-C2), and EGFP (Biotechne, cat no: 400281-C3) were applied to the sections and incubated for 2 hours at 40°C. Sections were then washed using the wash buffer, followed by an O/N incubation in 5x SSC.

The following day sections were washed in wash buffer, followed by application of 4 drops of Multiplex FL v2 AMP 1. Sections were incubated at 40°C for 30 minutes and washed using wash buffer afterwards. This step was repeated for Amp 2 and 3, with only a 15-minute incubation for Amp3. Following the last washing step, 4 drops of Multiplex HRP-C1 was applied to each section followed by incubation for 15 minutes at 40°C. Sections were washed using wash buffer, 150 µl Opal 620, diluted 1:1000 in TSA buffer, was added to each section and they were then incubated at 40°C for 30 minutes. Following incubation, the sections were washed with wash buffer, 4 drops of Multiplex FL v2 HRP blocker were added to each section and the slides were incubated at 40°C for 15 minutes. They were then washed in wash buffer. Everything in this paragraph was repeated, but using Amp2/Amp3, HRP-C1/HRP-C2, and Opal 690/Fluorescein. Following the last wash, a drop of PVA-DABCO with added DAPI (1:1000 dilution), was used to coverslip the sections. They were left O/N to dry.

Lentivirus production

Cells were seeded (roughly $12{,}5*10^6$ 293T cells in aT175) the day before transfection so that the confluency was 75-90% at time of transfection with 20 ml DMEM with Glutamax + 10%FBS + Penicillin (100 U/ml)/Streptomycin (100 µg/ml). Before transfection the medium was aspirated and 16.2 ml/T175 of new medium added.

For transfection using PEI, a total of 28 µg DNA and 84 µg PEI per T175 was mixed at a 5:4:1 ratio of the transgene plasmid, the packaging plasmid, and the envelope plasmid.

The DNA was diluted in DPBS or DMEM+P/S so that the total volume (including PEI) became 0.1x the culture medium volume, that is 1,8 ml.

PEI was added and the tube mixed by vortexing for a few seconds. The transfection mix was Incubated at room temperature for 15 minutes.

For transfection using Calcium Phosphate, viral production plasmids were mixed same as when using PEI. 0.1 x TE-buffer was then added up to a volume of 810 µl followed by addition of 90 µl of 2.5 M $CaCl_2$. The mix was put on a vortex and and 900 µl of 2 x HEBS was added dropwise with constant vortexing. The transfection mix was left for 5 minutes at RT and 1.8 ml was added to each flask.

The transfection mix was added to the cell culture by tilting the flask to gather the medium at the bottom and the transfection mix was added to the medium to prevent disrupting the cells attached to the bottom of the flask. After addition of the transfection mix, the flask was gently rocked back and forth to distribute the transfection mix evenly. The cells were incubated at 37°C at a 5% CO2 until harvest of medium.

Cell supernatant was collected 45 hours after transfection and another 18 ml of medium was added. The supernatant was centrifuged at 800 x g for 10 minutes, 4°C. The supernatant was filtered through a 0.45 µm pore size filter. The filtrate was transferred to a Beckman ultracentrifugation tube and centrifuged at 76500 x g for 1.5 hours at 4°C. After centrifugation the supernatant down to approximately 1 ml was discarded and the tube stored at 4°C O/N. The following day cell supernatant was collected again. The supernatant was centrifuged at 800 x g for 10 minutes, 4°C. The supernatant was filtered through a 0.45 µm pore size filter. The filtrate was transferred to the same Beckman ultracentrifugation tube used previously and centrifuged at 76500 x g for 1.5 hours at 4°C. The supernatant was discarded, and the virus-pellet was resuspended by adding cold PBS. The pellet was left to dissolve at 4°C at least 2 h or O/N. The virus was aliquoted and frozen at -80°C.

Lentivirus titration

Each batch was titered by quantitative PCR. The batches to be titered were used to transduce 100000 293T cells in each well of a 6-well plate. 3, 1 or 0.3 µl of the virus, diluted using DPBS, was added to each well. A reference batch expressing GFP was also added to one set of 3 wells using the same volumes. The reference batch had previously had its titer determined by quantification of the number of cells transduced and expressing GFP using a flow cytometer.

Primers targeting the human albumin gene as well as the WPRE sequence were used. The C_p value for each well was then calculated by the Lightcycler software. The values from the albumin primers were used to normalize the values from the WPRE primers, since the albumin gene should be present in the same number in each genome of the 293T cells. After normalization, the value was compared to the reference batch to calculate the predicted functional titer of the virus batch.

AAV production

Similarly to the LV production, cells were seeded (roughly 12,5 *$10^6$293T cells in aT175) the day before transfection so that the confluency was 75-90% at time of transfection. 27 ml of DMEM with Glutamax + 10%FBS + Penicillin (100 U/ml)/Streptomycin (100 µg/ml) was added to each flask.

Transfection was performed using PEI. 28 µg of plasmid DNA was mixed in 3ml DPBS at a ratio of 1.2:1:1 of transfer, helper, and capsid plasmid using a three-plasmid system, and 1:1 of transfer and helper plasmid using a two plasmid system. 84 µg of PEI was added to the plasmid mix, vortexed and incubated at RT. Following incubation, the transfection mix was added to the HEK 293T cells. 24 hours later 90% of the medium was aspirated and replaced with 27 ml Optipro.

48-72 hours after medium change virus was harvested. Cells were detached from flask using a cell-scraper and collected with the medium (volume should be 30 ml). 3 ml of chloroform was added to the cells and medium followed by 5 minutes of vortexing. After vortexing, 7.6 ml of NaCl was added to each tube and briefly vortexed. Tubes were centrifuged for 5 minutes at 3000 x *g* and 4°C. The aqueous phase (largest volume, upper phase) was then transferred to a new tube. 9.4 ml of 50% PEG 8000 was added to each tube, briefly vortexed, and incubated on ice for 1 hour.

Following incubation, the tubes were centrifuged for 30 minutes at 3000 x *g* and 4°C. The supernatant was discarded, and pellet resuspended in 1.4 ml of HEPES buffer. Following resuspension, 3.5 µl 1M MgCl2, 14 µl DNase I, and 1.4 µl RNase A was added to each tube. The tubes were briefly mixed and then incubated at 37°C for 20 minutes. Chloroform was added at a 1:1 ratio to the tubes, vortexed and then centrifuged for 5 minutes at 3000 x *g* and 4°C. The aqueous phase was transferred to a new tube and the process from addition of chloroform repeated three more times.

Following collection of the aqueous phase the last time, tubes were left with lid open for 30 minutes for evaporation of chloroform. The aqueous phase was then loaded onto 100000 kDa molecular weight cut-off ultrafiltration columns. The columns were centrifuged at 14000 x *g* at RT for 5 minutes. This step was repeated until all of the aqueous phase had been loaded onto the column. The flowthrough was discarded and the solution remaining in the column was diluted using 400 µl DPBS and centrifuged at 14000 x *g* at RT for 5 minutes. The dilution with DPBS and subsequent centrifugation was repeated 4 times. For the last centrifugation step the time was increased to 8 minutes. The column was then removed from the collection tube, inverted and placed into a new clean collection tube, which was centrifuged for 2 minutes at 1000 x *g* at RT. The AAV-containing DPBS solution was then transferred to a glass vial and stored at 4°C.

AAV titration

AAV was titered through lysis of AAV particles and ITR count through qPCR. 1 µl of the AAV batch to be tittered was diluted in 89 µl of PBS and 10 µl of 10x DNase I reaction buffer. 2 Units of DNase I was added, followed by incubation at 37°C for 10 minutes. In order to inactivate DNaseI, 1µl of 0.5M EDTA was added, and the sample incubated at 65°C for 10 minutes. To lyse the AAV, 1 µl (20µg) of Proteinase K was added followed by incubation at 50°C for 60 minutes. Proteinase K was heat inactivated by incubation at 95°C for 20 minutes.

A standard curve for qPCR was prepared by linearizing an AAV transfer plasmid, with a 10-fold dilution series from $1*10^9$ copy nr/µl to $1*10^3$ copy nr/µl. 1 µl of sample (standard curve or AAV-batch genomic DNA) was added to 4 µl of ITR targeting FAM-primer probes (0.5 µM final concentration of each primer), and 5 µl of SYBR Green Mastermix in a 384-well qPCR plate.

The thermocycler was run with the following settings: 98°C for 30 seconds, followed by 39 cycles of: 98°C for 5 seconds, and 60°C for 30 seconds. DNA quantities was measure using FAM-probes and C_p values calculated by the Lightcycler software. The standard curve was then used to determine the genome copies/ml of the AAV batches.

Western blot and total protein staining

LV samples were inactivated by adding 1% Tween 20 at a 1:1 ratio. AAV samples were diluted using DPBS to achieve a final amount of $5*10^9$ gc/well, and inactivation was performed through denaturation in the next step. Both AAV and LV samples were diluted in Laemmli buffer at a 1:1 ratio up to a total volume of 20 µl. The sample was heated up to 99°C for 5 minutes and then chilled on ice. For paper I, a TGX stain-free gel from Bio-Rad was washed with water and put in the electrophoresis system. The inner and outer chambers are filled with 200 ml and 600 ml TGS running buffer, respectively. 20 µl of sample was then loaded into the wells and the gel was run at 200 V for 30 minutes. After the run the gel was imaged by exposing it to UV-light for 1 minute and the fluorescence was measured. For paper II, a 4-12% Bis-Tris (Thermo Fisher Scientific) gel was used together with MOPS running buffer (Thermo Fisher Scientific). Gel was otherwise run under identical conditions, but without UV exposure after the run. The gel was either used for blotting, or total protein staining using Coomassie Brilliant Blue R-250 (only in paper II).

For gels used for western blotting, the proteins were then transferred to a PVDF membrane using the trans-blot turbo transfer system (Bio-Rad) and pre-made trans-blot turbo PVDF membrane sandwiches (Bio-Rad). Successful transfer was controlled

by imaging the PVDF membrane with UV-light for paper I, and through Ponceau S staining in paper II. The membrane was then washed using TTBS for 15 minutes followed by a 1 hour incubation with 5% milk powder solution. The blocking solution was then discarded, and the membrane washed in TTBS. Following the washing step, the membrane is incubated together with a-BSA antibody (Sigma, B-2901) in 5% milk powder solution. After primary antibody incubation the image is developed using a 5 minute incubation in ECL prime.

For total protein staining, the gel was briefly washed using distilled water and then incubated O/N at RT in 0.1% Coomassie Brilliant Blue R-250, 40% Methanol and 10% Acetic acid. The gel was de-stained the following day in 40% Methanol and 10% Acetic acid until bands were visible and then imaged.

Cell counting

For paper I, DAB-stained cells were counted manually using the Olympus AX70 at a magnification of 100x. Counting was performed from the section corresponding to plate 11 to plate 21 of the Paxinos and Watson second edition rat brain atlas. To get an estimation of the total number of cells present in this part of the brain, the method proposed by M. Abercrombie (Equation 1) was used. (Abercrombie, 1946)

$$P = A * \frac{M}{L + M}$$

Where P is the average number of cells, A is the number of counted cells, M is the thickness of the section and L is the length of the cell body. P was then multiplied by 6 to account for the fact that each brain was cut in series of 6.

For paper III, images of the sections of interest were taken using the Leica DMI 6000B and Leica DFC360FX at a 100x magnification. For the purpose of counting GFP^+ and $DARP32^+$ neurons, Images were split into green and blue channels and all labelled cells within the green channel in the striatum of a section were counted and marked. The blue channel was then used to count how many of the previously labelled cells were also blue.

In paper IV, images were taken using an Olympus AX70 at a magnification of 400x for DRD1/GFP staining or the Leica DMI 6000B and Leica DFC360FX at a 200x magnification for ChAT/mCherry staining. For quantification of DRD1- and GFP^+ cells, an area around the outside of the injection tract, containing transduced cells, but as few overlapping cells expressing GFP as possible, was chosen from different sections from the two animals injected. Images of these areas were converted into grayscale and

the "Enhance local Contrast (CLAHE)" (Zuiderveld, 1994) plugin for imagej (Rueden et al., 2017; Schindelin et al., 2012) used to aid in counting. GFP^+ cells within this area were marked. The DAPI channel was then controlled to ensure that GFP^+ cells marked would overlap with a nucleus. GFP^+ cells were then controlled for DRD1 overlap or lack thereof. In order to judge this, a GFP^+ cell which showed DRD1 staining that is darker within the GFP^+ area compared to its surroundings was considered DRD1 negative, whereas one that was similarly stained or completely covered was considered DRD1 positive.

$ChAT^+$ and $mCherry^+$ neurons were counted by splitting the red and green channels, marking the $mCherry^+$ cells and then the number of cells also $ChAT^+$. In order to count the number of $ChAT^+$ cells within the area of injection, but not stained for mCherry, red cells surrounded by green cells, or with more than a single green cell within 50-100 µm were counted.

Brains stained using RNAscope was imaged using a confocal microscope at a 100x magnification, with an emission filter that could be regulated to separate the Opal 620 and 690 emissions. GFP mRNA staining was localized (labelled with Fluorescein) and then checked for colocalization with either DRD1 mRNA staining (labelled with Opal 690), or Adora2a mRNA staining (labelled with Opal 620).

miRNA immunoprecipitation and RNA purification

200 µl Protein G Dynabeads were washed twice using PBST. 0.5 µg Antibody targeting GFP (ab6556, Abcam) diluted in 500 µl PBST was added to the beads. The beads were then incubated at RT for 1 hour with end-over-end rotation. The beads were then washed twice with PBST followed by two wash steps with miRNA lysis buffer.

During the 1 hour incubation, animals were sacrificed and brains extracted as previously described. The brain-pieces were immediately dropped into MP lysing matrix D 2 ml tubes containing 500 µl of complete lysis buffer and placed on ice. The samples were lysed using a MP Fastprep-24 at 5 m/s for 2x 1 minute. The lysate was transferred to an eppendorf tube and centrifuged at 4°C, 16200 x *g* for 15 minutes. After centrifugation, the supernatant was transferred to a new Eppendorf tube. 50 µl was saved from each sample. The remaining lysate was incubated with the Dynabeads at 4°C for 24 hours with end-over-end rotation. Following incubation, the beads were spun down and washed with low salt NT2 buffer. They were then washed twice with high salt NT2 buffer. With the last washing step done, the beads were resuspended with 700 µl QIAzol and incubated for 10 minutes at RT. The beads were collected using a magnet and the QIAzol containing the RNA transferred to a new Eppendorf tube. 140 µl of chloroform was added to each sample followed by 15 seconds of

vortexing. miRNA was then purified using the Qiagen miRNEasy micro kit according to the protocol for miRNA-enriched fractions, appendix A.

RT qPCR for miRNA

For paper I, the Qiagen miRCURY LNA miRNA starter kit was used for RT qPCR of extracted miRNA. RNA concentrations of samples were not measured due to the low amounts of RNA, but instead 6.5 µl was used for the cDNA reverse transcription. U6 spike-ins was used as controls for cDNA reverse transcription. Furthermore, the cDNA was only diluted 1:10 before qPCR. Primers targeting the mature miRNAs 21a-3p, 103-3p or 124-3p were used during qPCR. The kit was used following the protocol in all other regards. C_p values were calculated by the Roche Lightcycler 480 II instrument software.

smallRNA-seq

Library was prepared by J. G. Johansson using the NEXTFLEX small-RNA seq kit v3 for illumina sequencing. Due to the low amounts of RNA present after small RNA purifiction, the maximum amount of sample (10.5 µl) was used for library preparation. There was no size selection performed on the library before sequencing.

Bioinformatics

Trimming, mapping and counting of reads was performed by R. Garza. We used the edgeR R-package (Robinson, McCarthy, & Smyth, 2009) in order to analyse our samples for differential expression. MiRNA with less than 5 counts in at least two samples were removed and normalization factors for the libraries calculated using TMM (Robinson & Oshlack, 2010). For estimating dispersions we used the Cox-Reid profile-adjusted likelihood method (McCarthy, Chen, & Smyth, 2012). We then proceeded to test for DE using a quasi-likelihood F-test (Robinson et al., 2009). FDR was calculated using the Benjamini-Hochberg procedure (Benjamini & Hochberg, 1995).

Molecular cloning

The D2SP promoter was ordered as a GeneArt string, using the sequence given in (Zalocusky et al., 2016) inserted into a plasmid for cloning from Thermo Fisher Scientific. The D2SP promoter and a pscAAV.CMV.mCherry plasmid, kindly donated by Marcus Davidsson and Tomas Björklund, was restricted using AvrII and BamHI and then ligated to create the pAAV.D2SP.mCherry transfer plasmid.

The D2SP promoter was amplified through PCR and restriction sites for ClaI and AgeI added with the primers. Both the PCR fragment and the pLV.CMV.GFP-Ago2, kindly donated by Johan Jakobsson, was restricted using ClaI and AgeI and then ligated.

Similarly, the hSyn promoter was amplified through PCR and restriction sites for ClaI and BamHI added with the primers. Both the PCR fragment and the pLV.CMV.GFP-Ago2, kindly donated by Johan Jakobsson, was restricted using ClaI and BamHI and then ligated.

For the pAAV.hSyn.(loxp)CTE.GFP-Ago2 plasmid, pAAV.XK-EGFP-myc-Ago2, kindly donated by Johan Jakobsson, was opened and blunted upstream of the GFP-Ago2 fusion protein using AgeI. pscAAV.CTE-GFP, kindly donated by Marcus Davidsson and Tomas Björklund, was also restricted using AgeI to create an insert of the (loxp)CTE fragment and ends blunted. The backbone and insert were then ligated. Clones were checked for correct orientation of the insert. Plasmid maps for transfer plasmids used in thesis are shown in Figure 15 and 16.

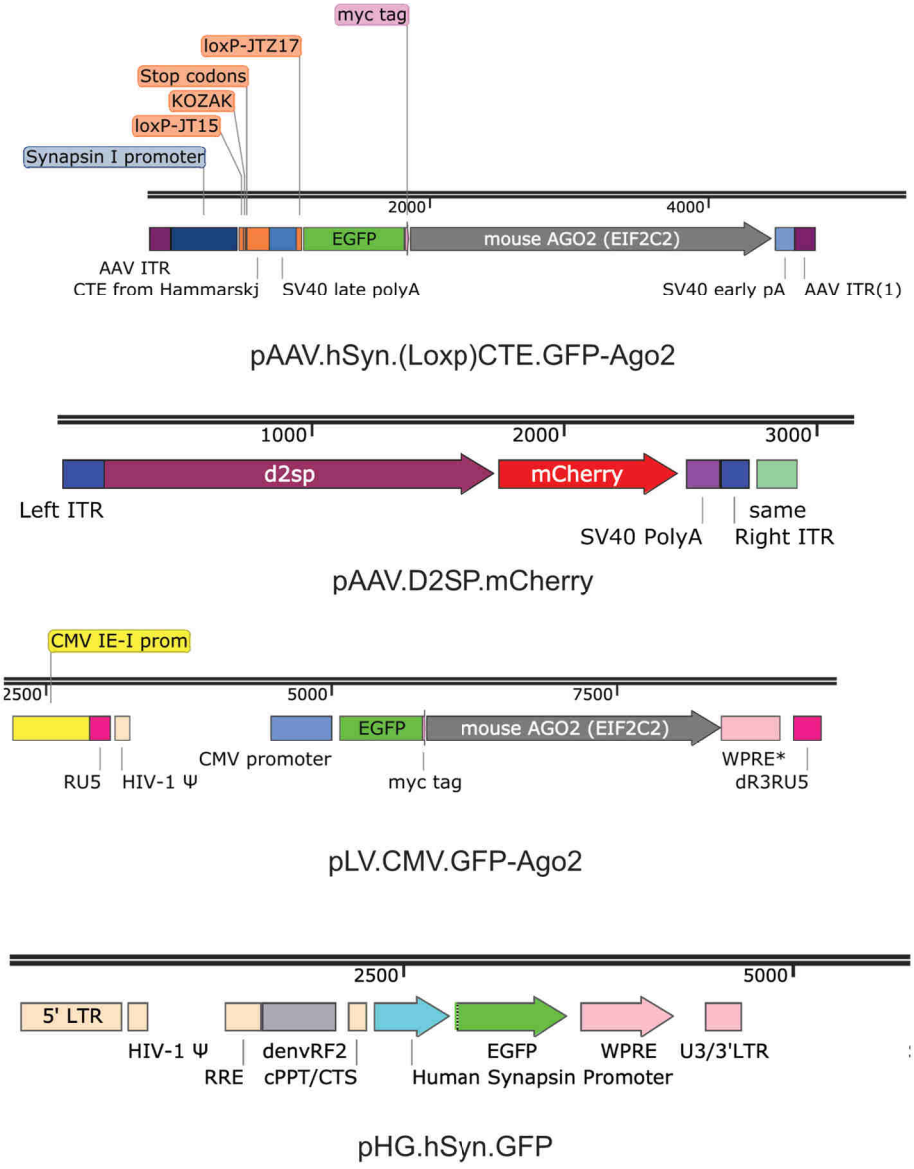

Figure 15: Plasmid maps of the different transfer vectors used in this thesis.

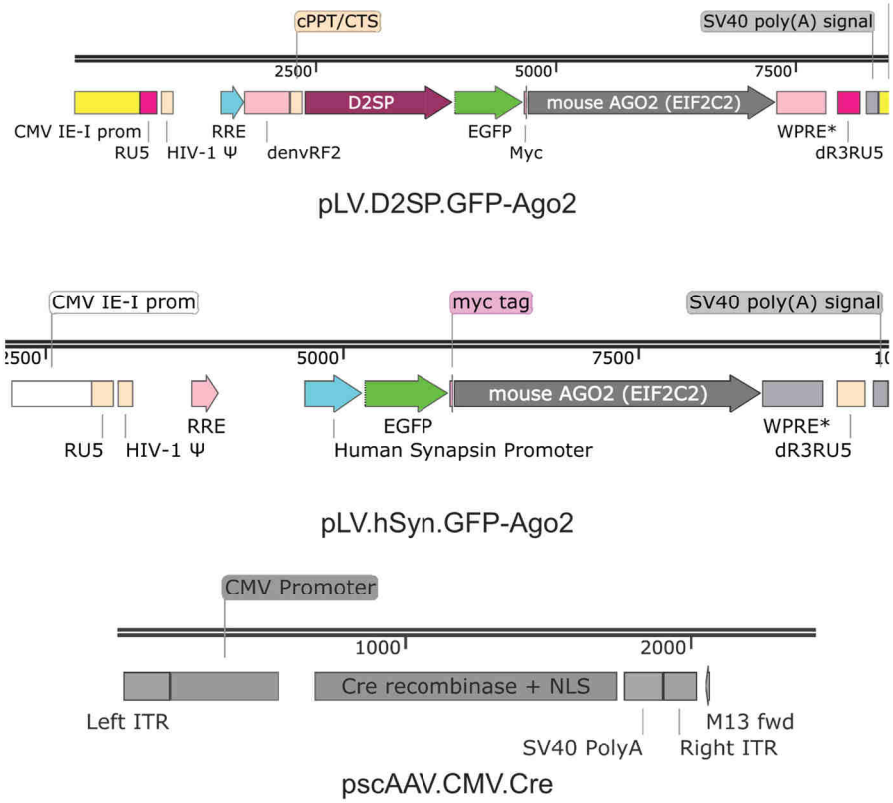

Figure 16: Plasmid maps of the different transfer vectors used in this thesis continued.

References

Abercrombie, M. (1946). Estimation of nuclear population from microtome sections. *Anat Rec, 94*, 239-247.

Agarwal, V., Bell, G. W., Nam, J.-W., & Bartel, D. P. (2015). Predicting effective microRNA target sites in mammalian mRNAs. *Elife, 4*. doi:10.7554/eLife.05005

Akerblom, M., Petri, R., Sachdeva, R., Klussendorf, T., Mattsson, B., Gentner, B., & Jakobsson, J. (2014). microRNA-125 distinguishes developmentally generated and adult-born olfactory bulb interneurons. *Development, 141*(7), 1580-1588. doi:10.1242/dev.101659

Akerblom, M., Sachdeva, R., Barde, I., Verp, S., Gentner, B., Trono, D., & Jakobsson, J. (2012). MicroRNA-124 Is a Subventricular Zone Neuronal Fate Determinant. *Journal of Neuroscience, 32*(26), 8879-8889. doi:10.1523/jneurosci.0558-12.2012

Alberti, C., Manzenreither, R. A., Sowemimo, I., Burkard, T. R., Wang, J., Mahofsky, K., . . . Cochella, L. (2018). Cell-type specific sequencing of microRNAs from complex animal tissues. *Nature methods, 15*(4), 283-289. doi:10.1038/nmeth.4610

Albin, R. L., Young, A. B., & Penney, J. B. (1989). The functional anatomy of basal ganglia disorders. *Trends in Neurosciences, 12*(10), 366-375. doi:10.1016/0166-2236(89)90074-x

Alcacer, C., Andreoli, L., Sebastianutto, I., Jakobsson, J., Fieblinger, T., & Cenci, M. A. (2017). Chemogenetic stimulation of striatal projection neurons modulates responses to Parkinson's disease therapy. *Journal of Clinical Investigation, 127*(2), 720-734. doi:10.1172/jci90132

Alexander, G. E., & Crutcher, M. D. (1990). Functional architecture of basal ganglia circuits: neural substrates of parallel processing. *Trends in Neurosciences, 13*(7), 266-271. doi:10.1016/0166-2236(90)90107-l

Ambros, V. (2004). The functions of animal microRNAs. *Nature, 431*(7006), 350-355. doi:10.1038/nature02871

Atchison, R. W., Casto, B. C., & Hammon, W. M. (1965). Adenovirus-Associated Defective Virus Particles. *Science, 149*(3685), 754-755. doi:10.1126/science.149.3685.754

Baba, M., Nakajo, S., Tu, P. H., Tomita, T., Nakaya, K., Lee, V. M., . . . Iwatsubo, T. (1998). Aggregation of alpha-synuclein in Lewy bodies of sporadic Parkinson's disease and dementia with Lewy bodies. *Am J Pathol, 152*(4), 879-884.

Babiarz, J. E., Hsu, R., Melton, C., Thomas, M., Ullian, E. M., & Blelloch, R. (2011). A role for noncanonical microRNAs in the mammalian brain revealed by phenotypic differences in Dgcr8 versus Dicer1 knockouts and small RNA sequencing. *RNA, 17*(8), 1489-1501. doi:10.1261/rna.2442211

Babiarz, J. E., Ruby, J. G., Wang, Y., Bartel, D. P., & Blelloch, R. (2008). Mouse ES cells express endogenous shRNAs, siRNAs, and other Microprocessor-independent, Dicer-dependent small RNAs. *Genes & development, 22*(20), 2773-2785. doi:10.1101/gad.1705308

Baekelandt, V., Eggermont, K., Michiels, M., Nuttin, B., & Debyser, Z. (2003). Optimized lentiviral vector production and purification procedure prevents immune response after transduction of mouse brain. *Gene therapy, 10*(23), 1933-1940. doi:10.1038/sj.gt.3302094

Bai, X., Tang, Y., Yu, M., Wu, L., Liu, F., Ni, J., . . . Wang, J. (2017). Downregulation of blood serum microRNA 29 family in patients with Parkinson's disease. *Scientific reports, 7*(1). doi:10.1038/s41598-017-03887-3

Bardelli, M., Zárate-Pérez, F., Agúndez, L., Linden, R. M., Escalante, C. R., Henckaerts, E., & Banks, L. (2016). Identification of a Functionally Relevant Adeno-Associated Virus Rep68 Oligomeric Interface. *Journal of virology, 90*(15), 6612-6624. doi:10.1128/jvi.00356-16

Barnes, C., Scheideler, O., & Schaffer, D. (2019). Engineering the AAV capsid to evade immune responses. *Current Opinion in Biotechnology, 60*, 99-103. doi:10.1016/j.copbio.2019.01.002

Bates, G. P., Dorsey, R., Gusella, J. F., Hayden, M. R., Kay, C., Leavitt, B. R., . . . Tabrizi, S. J. (2015). Huntington disease. *Nature Reviews Disease Primers, 1*(1). doi:10.1038/nrdp.2015.5

Bateup, H. S., Santini, E., Shen, W., Birnbaum, S., Valjent, E., Surmeier, D. J., . . . Greengard, P. (2010). Distinct subclasses of medium spiny neurons differentially regulate striatal motor behaviors. *Proceedings of the National Academy of Sciences, 107*(33), 14845-14850. doi:10.1073/pnas.1009874107

Behm-Ansmant, I. (2006). mRNA degradation by miRNAs and GW182 requires both CCR4:NOT deadenylase and DCP1:DCP2 decapping complexes. *Genes & development, 20*(14), 1885-1898. doi:10.1101/gad.1424106

Benjamini, Y., & Hochberg, Y. (1995). Controlling the False Discovery Rate: A Practical and Powerful Approach to Multiple Testing. *Journal of the Royal Statistical Society. Series B (Methodological), 57*(1), 289-300.

Bernstein, E., Kim, S. Y., Carmell, M. A., Murchison, E. P., Alcorn, H., Li, M. Z., . . . Hannon, G. J. (2003). Dicer is essential for mouse development. *Nature Genetics, 35*(3), 215-217. doi:10.1038/ng1253

Bian, S., Hong, J., Li, Q., Schebelle, L., Pollock, A., Knauss, Jennifer L., . . . Sun, T. (2013). MicroRNA Cluster miR-17-92 Regulates Neural Stem Cell Expansion and Transition to Intermediate Progenitors in the Developing Mouse Neocortex. *Cell reports, 3*(5), 1398-1406. doi:10.1016/j.celrep.2013.03.037

Björklund, A., & Dunnett, S. B. (2019). The Amphetamine Induced Rotation Test: A Re-Assessment of Its Use as a Tool to Monitor Motor Impairment and Functional Recovery in Rodent Models of Parkinson's Disease. *Journal of Parkinson's Disease, 9*(1), 17-29. doi:10.3233/jpd-181525

Borchelt, D. R., Marcellin, D., Abramowski, D., Young, D., Richter, J., Weiss, A., . . . Lotz, G. P. (2012). Fragments of HdhQ150 Mutant Huntingtin Form a Soluble Oligomer Pool That Declines with Aggregate Deposition upon Aging. *PloS one, 7*(9). doi:10.1371/journal.pone.0044457

Borger, E., Herrmann, A., Mann, D. A., Spires-Jones, T., & Gunn-Moore, F. (2014). The Calcium-Binding Protein EFhd2 Modulates Synapse Formation In Vitro and Is Linked to Human Dementia. *Journal of Neuropathology & Experimental Neurology, 73*(12), 1166-1182. doi:10.1097/nen.0000000000000138

Botta-Orfila, T., Morató, X., Compta, Y., Lozano, J. J., Falgàs, N., Valldeoriola, F., . . . Ezquerra, M. (2014). Identification of blood serum micro-RNAs associated with idiopathic andLRRK2Parkinson's disease. *Journal of Neuroscience Research, 92*(8), 1071-1077. doi:10.1002/jnr.23377

Brown, J. T., Planert, H., Berger, T. K., & Silberberg, G. (2013). Membrane Properties of Striatal Direct and Indirect Pathway Neurons in Mouse and Rat Slices and Their Modulation by Dopamine. *PloS one, 8*(3). doi:10.1371/journal.pone.0057054

Burchett, S. A., Bannon, M. J., & Granneman, J. G. (2001). RGS mRNA Expression in Rat Striatum. *Journal of neurochemistry, 72*(4), 1529-1533. doi:10.1046/j.1471-4159.1999.721529.x

Cao, X.-Y., Lu, J.-M., Zhao, Z.-Q., Li, M.-C., Lu, T., An, X.-S., & Xue, L.-J. (2017). MicroRNA biomarkers of Parkinson's disease in serum exosome-like microvesicles. *Neuroscience Letters, 644*, 94-99. doi:10.1016/j.neulet.2017.02.045

Cazorla, M., de Carvalho, F. D., Chohan, M. O., Shegda, M., Chuhma, N., Rayport, S., . . . Kellendonk, C. (2014). Dopamine D2 receptors regulate the anatomical and functional balance of basal ganglia circuitry. *Neuron, 81*(1), 153-164. doi:10.1016/j.neuron.2013.10.041

Chang, L. S., Shi, Y., & Shenk, T. (1989). Adeno-associated virus P5 promoter contains an adenovirus E1A-inducible element and a binding site for the major late transcription factor. *Journal of virology, 63*(8), 3479-3488. doi:10.1128/jvi.63.8.3479-3488.1989

Colgan, L. A., Hu, M., Misler, J. A., Parra-Bueno, P., Moran, C. M., Leitges, M., & Yasuda, R. (2018). PKCα integrates spatiotemporally distinct Ca2+ and autocrine BDNF signaling to facilitate synaptic plasticity. *Nature Neuroscience, 21*(8), 1027-1037. doi:10.1038/s41593-018-0184-3

Connolly, B. S., & Lang, A. E. (2014). Pharmacological Treatment of Parkinson Disease. *Jama, 311*(16). doi:10.1001/jama.2014.3654

Cuellar, T. L., Davis, T. H., Nelson, P. T., Loeb, G. B., Harfe, B. D., Ullian, E., & McManus, M. T. (2008). Dicer loss in striatal neurons produces behavioral and neuroanatomical phenotypes in the absence of neurodegeneration. *Proceedings of the National Academy of Sciences, 105*(14), 5614-5619. doi:10.1073/pnas.0801689105

Cui, G., Jun, S. B., Jin, X., Pham, M. D., Vogel, S. S., Lovinger, D. M., & Costa, R. M. (2013). Concurrent activation of striatal direct and indirect pathways during action initiation. *Nature, 494*(7436), 238-242. doi:10.1038/nature11846

Davidsson, M., Wang, G., Aldrin-Kirk, P., Cardoso, T., Nolbrant, S., Hartnor, M., . . . Björklund, T. (2019). A systematic capsid evolution approach performed in vivo for the design of AAV vectors with tailored properties and tropism. *Proceedings of the National Academy of Sciences, 116*(52), 27053-27062. doi:10.1073/pnas.1910061116

Davis, T. H., Cuellar, T. L., Koch, S. M., Barker, A. J., Harfe, B. D., McManus, M. T., & Ullian, E. M. (2008). Conditional Loss of Dicer Disrupts Cellular and Tissue Morphogenesis in the Cortex and Hippocampus. *Journal of Neuroscience, 28*(17), 4322-4330. doi:10.1523/jneurosci.4815-07.2008

de Almeida, L. P., Zala, D., Aebischer, P., & Deglon, N. (2001). Neuroprotective effect of a CNTF-expressing lentiviral vector in the quinolinic acid rat model of Huntington's disease. *Neurobiology of disease, 8*(3), 433-446. doi:10.1006/nbdi.2001.0388

Deeks, S. G., Overbaugh, J., Phillips, A., & Buchbinder, S. (2015). HIV infection. *Nature Reviews Disease Primers, 1*(1). doi:10.1038/nrdp.2015.35

DeLong, M. R., & Wichmann, T. (2007). Circuits and Circuit Disorders of the Basal Ganglia. *Archives of Neurology, 64*(1). doi:10.1001/archneur.64.1.20

Deng, Y.-P., Lei, W.-L., & Reiner, A. (2006). Differential perikaryal localization in rats of D1 and D2 dopamine receptors on striatal projection neuron types identified by retrograde labeling. *Journal of Chemical Neuroanatomy, 32*(2-4), 101-116. doi:10.1016/j.jchemneu.2006.07.001

Dull, T., Zufferey, R., Kelly, M., Mandel, R. J., Nguyen, M., Trono, D., & Naldini, L. (1998). A Third-Generation Lentivirus Vector with a Conditional Packaging System. *Journal of virology, 72*(11), 8463-8471. doi:10.1128/jvi.72.11.8463-8471.1998

Dzamko, N., Zhou, J., Huang, Y., & Halliday, G. M. (2014). Parkinsonâ€™s disease-implicated kinases in the brain; insights into disease pathogenesis. *Frontiers in Molecular Neuroscience, 7*. doi:10.3389/fnmol.2014.00057

Eilam, D., & Szechtman, H. (1989). Biphasic effect of D-2 agonist quinpirole on locomotion and movements. *European Journal of Pharmacology, 161*(2-3), 151-157. doi:10.1016/0014-2999(89)90837-6

Eulalio, A., Huntzinger, E., & Izaurralde, E. (2008). GW182 interaction with Argonaute is essential for miRNA-mediated translational repression and mRNA decay. *Nature structural & molecular biology, 15*(4), 346-353. doi:10.1038/nsmb.1405

Fabian, M. R., Sonenberg, N., & Filipowicz, W. (2010). Regulation of mRNA translation and stability by microRNAs. *Annu Rev Biochem, 79*, 351-379. doi:10.1146/annurev-biochem-060308-103103

Ficblinger, T., Sebastianutto, I., Alcacer, C., Bimpisidis, Z., Maslava, N., Sandberg, S., . . . Cenci, M. A. (2014). Mechanisms of Dopamine D1 Receptor-Mediated ERK1/2 Activation in the Parkinsonian Striatum and Their Modulation by Metabotropic Glutamate Receptor Type 5. *Journal of Neuroscience, 34*(13), 4728-4740. doi:10.1523/jneurosci.2702-13.2014

Fieblinger, T., Zanetti, L., Sebastianutto, I., Breger, L. S., Quintino, L., Lockowandt, M., . . . Cenci, M. A. (2018). Striatonigral neurons divide into two distinct morphological-physiological phenotypes after chronic L-DOPA treatment in parkinsonian rats. *Scientific reports, 8*(1). doi:10.1038/s41598-018-28273-5

Finnerty, J. R., Wang, W. X., Hebert, S. S., Wilfred, B. R., Mao, G., & Nelson, P. T. (2010). The miR-15/107 group of microRNA genes: evolutionary biology, cellular functions, and roles in human diseases. *J Mol Biol, 402*(3), 491-509. doi:10.1016/j.jmb.2010.07.051

Frederick, A. L., Yano, H., Trifilieff, P., Vishwasrao, H. D., Biezonski, D., Mészáros, J., . . . Javitch, J. A. (2015). Evidence against dopamine D1/D2 receptor heteromers. *Molecular Psychiatry, 20*(11), 1373-1385. doi:10.1038/mp.2014.166

Friedman, R. C., Farh, K. K. H., Burge, C. B., & Bartel, D. P. (2008). Most mammalian mRNAs are conserved targets of microRNAs. *Genome research, 19*(1), 92-105. doi:10.1101/gr.082701.108

Fujiyama, F., Sohn, J., Nakano, T., Furuta, T., Nakamura, K. C., Matsuda, W., & Kaneko, T. (2011). Exclusive and common targets of neostriatofugal projections of rat striosome neurons: a single neuron-tracing study using a viral vector. *European Journal of Neuroscience, 33*(4), 668-677. doi:10.1111/j.1460-9568.2010.07564.x

George, S. R., O'Dowd, B. F., Hasbi, A., & Perreault, M. L. (2011). The Dopamine D1–D2 Receptor Heteromer in Striatal Medium Spiny Neurons: Evidence for a Third Distinct Neuronal Pathway in Basal Ganglia. *Frontiers in Neuroanatomy, 5*. doi:10.3389/fnana.2011.00031

Gerfen, C., Engber, T., Mahan, L., Susel, Z., Chase, T., Monsma, F., & Sibley, D. (1990). D1 and D2 dopamine receptor-regulated gene expression of striatonigral and striatopallidal neurons. *Science, 250*(4986), 1429-1432. doi:10.1126/science.2147780

Gertler, T. S., Chan, C. S., & Surmeier, D. J. (2008). Dichotomous Anatomical Properties of Adult Striatal Medium Spiny Neurons. *Journal of Neuroscience, 28*(43), 10814-10824. doi:10.1523/jneurosci.2660-08.2008

Giraldez, M. D., Spengler, R. M., Etheridge, A., Godoy, P. M., Barczak, A. J., Srinivasan, S., . . . Tewari, M. (2018). Comprehensive multi-center assessment of small RNA-seq methods for quantitative miRNA profiling. *Nature Biotechnology, 36*(8), 746-757. doi:10.1038/nbt.4183

Girod, A., Ried, M., Wobus, C., Lahm, H., Leike, K., Kleinschmidt, J., . . . Hallek, M. (1999). Genetic capsid modifications allow efficient re-targeting of adeno-associated virus type 2. *Nature medicine, 5*(9), 1052-1056. doi:10.1038/12491

Gokce, O., Stanley, G. M., Treutlein, B., Neff, N. F., Camp, J. G., Malenka, R. C., . . . Quake, S. R. (2016). Cellular Taxonomy of the Mouse Striatum as Revealed by Single-Cell RNA-Seq. *Cell reports, 16*(4), 1126-1137. doi:10.1016/j.celrep.2016.06.059

Groiss, S. J., Wojtecki, L., Südmeyer, M., & Schnitzler, A. (2009). Review: Deep brain stimulation in Parkinson's disease. *Therapeutic Advances in Neurological Disorders, 2*(6), 379-391. doi:10.1177/1756285609339382

Group, H. S. (2006). Tetrabenazine as antichorea therapy in Huntington disease: A randomized controlled trial. *Neurology, 66*(3), 366-372. doi:10.1212/01.wnl.0000198586.85250.13

Gusella, J. F., MacDonald, M. E., & Lee, J.-M. (2014). Genetic modifiers of Huntington's disease. *Movement Disorders, 29*(11), 1359-1365. doi:10.1002/mds.26001

Han, J. (2004). The Drosha-DGCR8 complex in primary microRNA processing. *Genes & development, 18*(24), 3016-3027. doi:10.1101/gad.1262504

Han, L., Tang, Y., Bai, X., Liang, X., Fan, Y., Shen, Y., . . . Wang, J. (2020). Association of the serum microRNA-29 family with cognitive impairment in Parkinson's disease. *Aging, 12*(13), 13518-13528. doi:10.18632/aging.103458

Hanlon, K. S., Kleinstiver, B. P., Garcia, S. P., Zaborowski, M. P., Volak, A., Spirig, S. E., . . . György, B. (2019). High levels of AAV vector integration into CRISPR-induced DNA breaks. *Nature communications, 10*(1). doi:10.1038/s41467-019-12449-2

Hasbi, A., Nguyen, T., Rahal, H., Manduca, J. D., Miksys, S., Tyndale, R. F., . . . George, S. R. (2020). Sex difference in dopamine D1-D2 receptor complex expression and signaling affects depression- and anxiety-like behaviors. *Biology of Sex Differences, 11*(1). doi:10.1186/s13293-020-00285-9

Hasbi, A., Perreault, M. L., Shen, M. Y. F., Zhang, L., To, R., Fan, T., . . . George, S. R. (2014). A peptide targeting an interaction interface disrupts the dopamine D1-D2 receptor heteromer to block signaling and function in vitro and in vivo: effective selective antagonism. *The FASEB Journal, 28*(11), 4806-4820. doi:10.1096/fj.14-254037

He, M., Liu, Y., Wang, X., Zhang, Michael Q., Hannon, G. J., & Huang, Z. J. (2012). Cell-Type-Based Analysis of MicroRNA Profiles in the Mouse Brain. *Neuron, 73*(1), 35-48. doi:10.1016/j.neuron.2011.11.010

Hernández-López, S., Tkatch, T., Perez-Garci, E., Galarraga, E., Bargas, J., Hamm, H., & Surmeier, D. J. (2000). D2Dopamine Receptors in Striatal Medium Spiny Neurons Reduce L-Type Ca2+Currents and Excitability via a Novel PLCβ1–IP3–Calcineurin-Signaling Cascade. *The Journal of Neuroscience, 20*(24), 8987-8995. doi:10.1523/jneurosci.20-24-08987.2000

Hida, N., Aboukilila, M. Y., Burow, D. A., Paul, R., Greenberg, M. M., Fazio, M., . . . Cleary, M. D. (2017). EC-tagging allows cell type-specific RNA analysis. *Nucleic acids research, 45*(15), e138-e138. doi:10.1093/nar/gkx551

Hirano, M., Kato, S., Kobayashi, K., Okada, T., Yaginuma, H., & Kobayashi, K. (2013). Highly efficient retrograde gene transfer into motor neurons by a lentiviral vector pseudotyped with fusion glycoprotein. *PloS one, 8*(9), e75896. doi:10.1371/journal.pone.0075896

Ho, P. L., Michelfelder, S., Kohlschütter, J., Skorupa, A., Pfennings, S., Müller, O., . . . Trepel, M. (2009). Successful Expansion but Not Complete Restriction of Tropism of Adeno-Associated Virus by In Vivo Biopanning of Random Virus Display Peptide Libraries. *PloS one, 4*(4). doi:10.1371/journal.pone.0005122

Hoggan, M. D., Blacklow, N. R., & Rowe, W. P. (1966). Studies of small DNA viruses found in various adenovirus preparations: physical, biological, and immunological characteristics. *Proceedings of the National Academy of Sciences, 55*(6), 1467-1474. doi:10.1073/pnas.55.6.1467

Hu, W. S., & Hughes, S. H. (2012). HIV-1 Reverse Transcription. *Cold Spring Harbor Perspectives in Medicine, 2*(10), a006882-a006882. doi:10.1101/cshperspect.a006882

Huang, Y., Shen, X. J., Zou, Q., Wang, S. P., Tang, S. M., & Zhang, G. Z. (2011). Biological functions of microRNAs: a review. *Journal of physiology and biochemistry, 67*(1), 129-139. doi:10.1007/s13105-010-0050-6

Hubstenberger, A., Courel, M., Bénard, M., Souquere, S., Ernoult-Lange, M., Chouaib, R., . . . Weil, D. (2017). P-Body Purification Reveals the Condensation of Repressed mRNA Regulons. *Molecular cell, 68*(1), 144-157.e145. doi:10.1016/j.molcel.2017.09.003

Im, D.-S., & Muzyczka, N. (1990). The AAV origin binding protein Rep68 is an ATP-dependent site-specific endonuclease with DNA helicase activity. *Cell, 61*(3), 447-457. doi:10.1016/0092-8674(90)90526-k

Iwasaki, S., Kawamata, T., & Tomari, Y. (2009). Drosophila Argonaute1 and Argonaute2 Employ Distinct Mechanisms for Translational Repression. *Molecular cell, 34*(1), 58-67. doi:10.1016/j.molcel.2009.02.010

Jankovic, J. (2008). Parkinson's disease: clinical features and diagnosis. *J Neurol Neurosurg Psychiatry, 79*(4), 368-376. doi:10.1136/jnnp.2007.131045

Jin, X., Tecuapetla, F., & Costa, R. M. (2014). Basal ganglia subcircuits distinctively encode the parsing and concatenation of action sequences. *Nature Neuroscience, 17*(3), 423-430. doi:10.1038/nn.3632

Joglekar, A. V., & Sandoval, S. (2017). Pseudotyped Lentiviral Vectors: One Vector, Many Guises. *Human Gene Therapy Methods, 28*(6), 291-301. doi:10.1089/hgtb.2017.084

Johnson, R., Zuccato, C., Belyaev, N. D., Guest, D. J., Cattaneo, E., & Buckley, N. J. (2008). A microRNA-based gene dysregulation pathway in Huntington's disease. *Neurobiology of disease, 29*(3), 438-445. doi:10.1016/j.nbd.2007.11.001

Jovicic, A., Roshan, R., Moisoi, N., Pradervand, S., Moser, R., Pillai, B., & Luthi-Carter, R. (2013). Comprehensive expression analyses of neural cell-type-specific miRNAs identify new determinants of the specification and maintenance of neuronal phenotypes. *J Neurosci, 33*(12), 5127-5137. doi:10.1523/JNEUROSCI.0600-12.2013

Kafri, T., Blömer, U., Peterson, D. A., Gage, F. H., & Verma, I. M. (1997). Sustained expression of genes delivered directly into liver and muscle by lentiviral vectors. *Nature Genetics, 17*(3), 314-317. doi:10.1038/ng1197-314

Kato, S., Kobayashi, K., Inoue, K., Kuramochi, M., Okada, T., Yaginuma, H., . . . Kobayashi, K. (2011). A lentiviral strategy for highly efficient retrograde gene transfer by pseudotyping with fusion envelope glycoprotein. *Human gene therapy, 22*(2), 197-206. doi:10.1089/hum.2009.179

Kato, S., Kuramochi, M., Kobayashi, K., Fukabori, R., Okada, K., Uchigashima, M., . . . Kobayashi, K. (2011). Selective neural pathway targeting reveals key roles of thalamostriatal projection in the control of visual discrimination. *J Neurosci, 31*(47), 17169-17179. doi:10.1523/JNEUROSCI.4005-11.2011

Kawase-Koga, Y., Otaegi, G., & Sun, T. (2009). Different timings of dicer deletion affect neurogenesis and gliogenesis in the developing mouse central nervous system. *Developmental Dynamics, 238*(11), 2800-2812. doi:10.1002/dvdy.22109

Keaveney, M. K., Tseng, H.-a., Ta, T. L., Gritton, H. J., Man, H.-Y., & Han, X. (2018). A MicroRNA-Based Gene-Targeting Tool for Virally Labeling Interneurons in the Rodent Cortex. *Cell reports, 24*(2), 294-303. doi:10.1016/j.celrep.2018.06.049

Kim, J., Inoue, K., Ishii, J., Vanti, W. B., Voronov, S. V., Murchison, E., . . . Abeliovich, A. (2007). A MicroRNA Feedback Circuit in Midbrain Dopamine Neurons. *Science, 317*(5842), 1220-1224. doi:10.1126/science.1140481

Kim, W., Lee, Y., McKenna, N. D., Yi, M., Simunovic, F., Wang, Y., . . . Sonntag, K. C. (2014). miR-126 contributes to Parkinson's disease by dysregulating the insulin-like growth factor/phosphoinositide 3-kinase signaling. *Neurobiology of Aging, 35*(7), 1712-1721. doi:10.1016/j.neurobiolaging.2014.01.021

King, J. A. (2001). DNA helicase-mediated packaging of adeno-associated virus type 2 genomes into preformed capsids. *The EMBO journal, 20*(12), 3282-3291. doi:10.1093/emboj/20.12.3282

Klaus, A., Alves da Silva, J., & Costa, R. M. (2019). What, If, and When to Move: Basal Ganglia Circuits and Self-Paced Action Initiation. *Annual Review of Neuroscience, 42*(1), 459-483. doi:10.1146/annurev-neuro-072116-031033

Kravitz, A. V., Freeze, B. S., Parker, P. R. L., Kay, K., Thwin, M. T., Deisseroth, K., & Kreitzer, A. C. (2010). Regulation of parkinsonian motor behaviours by optogenetic control of basal ganglia circuitry. *Nature, 466*(7306), 622-626. doi:10.1038/nature09159

Kugler, S., Kilic, E., & Bahr, M. (2003). Human synapsin 1 gene promoter confers highly neuron-specific long-term transgene expression from an adenoviral vector in the adult rat brain depending on the transduced area. *Gene therapy, 10*(4), 337-347. doi:10.1038/sj.gt.3301905

Lee, J., Wang, W. G., & Sabatini, B. L. (2020). Anatomically segregated basal ganglia pathways allow parallel behavioral modulation. *Nature Neuroscience, 23*(11), 1388-+. doi:10.1038/s41593-020-00712-5

Lee, Kea J., Lee, Y., Rozeboom, A., Lee, J.-Y., Udagawa, N., Hoe, H.-S., & Pak, Daniel T. S. (2011). Requirement for Plk2 in Orchestrated Ras and Rap Signaling, Homeostatic Structural Plasticity, and Memory. *Neuron, 69*(5), 957-973. doi:10.1016/j.neuron.2011.02.004

Lee, R. C., Feinbaum, R. L., & Ambros, V. (1993). The C. elegans heterochronic gene lin-4 encodes small RNAs with antisense complementarity to lin-14. *Cell, 75*(5), 843-854.

Lee, S.-M., Kant, A., Blake, D., Murthy, V., Boyd, K., Wyrick, S. J., & Mailman, R. B. (2014). SKF-83959 is not a highly-biased functionally selective D1 dopamine receptor ligand with activity at phospholipase C. *Neuropharmacology, 86*, 145-154. doi:10.1016/j.neuropharm.2014.05.042

Lee, Y., Kim, M., Han, J., Yeom, K.-H., Lee, S., Baek, S. H., & Kim, V. N. (2004). MicroRNA genes are transcribed by RNA polymerase II. *The EMBO journal, 23*(20), 4051-4060. doi:10.1038/sj.emboj.7600385

Leitges, M., Kovac, J., Plomann, M., & Linden, D. J. (2004). A Unique PDZ Ligand in PKCα Confers Induction of Cerebellar Long-Term Synaptic Depression. *Neuron, 44*(4), 585-594. doi:10.1016/j.neuron.2004.10.024

Leterrier, C. (2018). The Axon Initial Segment: An Updated Viewpoint. *J Neurosci, 38*(9), 2135-2145. doi:10.1523/JNEUROSCI.1922-17.2018

Lim, L. P., Lau, N. C., Garrett-Engele, P., Grimson, A., Schelter, J. M., Castle, J., . . . Johnson, J. M. (2005). Microarray analysis shows that some microRNAs downregulate large numbers of target mRNAs. *Nature, 433*(7027), 769-773. doi:10.1038/nature03315

Liu, J. (2004). Argonaute2 Is the Catalytic Engine of Mammalian RNAi. *Science, 305*(5689), 1437-1441. doi:10.1126/science.1102513

Lopez, A., Munoz, A., Guerra, M. J., & Labandeira-Garcia, J. L. (2001). Mechanisms of the effects of exogenous levodopa on the dopamine-denervated striatum. *Neuroscience, 103*(3), 639-651.

Lusby, E., Fife, K. H., & Berns, K. I. (1980). Nucleotide sequence of the inverted terminal repetition in adeno-associated virus DNA. *Journal of virology, 34*(2), 402-409.

Maciotta, S., Meregalli, M., & Torrente, Y. (2013). The involvement of microRNAs in neurodegenerative diseases. *Frontiers in cellular neuroscience, 7*. doi:10.3389/fncel.2013.00265

Malmevik, J., Petri, R., Klussendorf, T., Knauff, P., Akerblom, M., Johansson, J., . . . Jakobsson, J. (2015). Identification of the miRNA targetome in hippocampal neurons using RIP-seq. *Scientific reports, 5*, 12609. doi:10.1038/srep12609

Margis, R., Margis, R., & Rieder, C. R. M. (2011). Identification of blood microRNAs associated to Parkinsońs disease. *Journal of Biotechnology, 152*(3), 96-101. doi:10.1016/j.jbiotec.2011.01.023

Matsushima, W., Herzog, V. A., Neumann, T., Gapp, K., Zuber, J., Ameres, S. L., & Miska, E. A. (2018). SLAM-ITseq: sequencing cell type-specific transcriptomes without cell sorting. *Development, 145*(13). doi:10.1242/dev.164640

McCarthy, D. J., Chen, Y., & Smyth, G. K. (2012). Differential expression analysis of multifactor RNA-Seq experiments with respect to biological variation. *Nucleic acids research, 40*(10), 4288-4297. doi:10.1093/nar/gks042

McCarty, D. M., Young, S. M., & Samulski, R. J. (2004). Integration of Adeno-Associated Virus (AAV) and Recombinant AAV Vectors. *Annual review of genetics, 38*(1), 819-845. doi:10.1146/annurev.genet.37.110801.143717

McColgan, P., & Tabrizi, S. J. (2018). Huntington's disease: a clinical review. *European Journal of Neurology, 25*(1), 24-34. doi:10.1111/ene.13413

McGeorge, A. J., & Faull, R. L. M. (1989). The organization of the projection from the cerebral cortex to the striatum in the rat. *Neuroscience, 29*(3), 503-537. doi:10.1016/0306-4522(89)90128-0

McLoughlin, H. S., Fineberg, S. K., Ghosh, L. L., Tecedor, L., & Davidson, B. L. (2012). Dicer is required for proliferation, viability, migration and differentiation in corticoneurogenesis. *Neuroscience, 223*, 285-295. doi:10.1016/j.neuroscience.2012.08.009

Meier, A. F., Fraefel, C., & Seyffert, M. (2020). The Interplay between Adeno-Associated Virus and Its Helper Viruses. *Viruses, 12*(6). doi:10.3390/v12060662

Meireles, J., & Massano, J. (2012). Cognitive impairment and dementia in Parkinson's disease: clinical features, diagnosis, and management. *Front Neurol, 3*, 88. doi:10.3389/fneur.2012.00088

Mercuri, N. B., & Bernardi, G. (2005). The 'magic' of L-dopa: why is it the gold standard Parkinson's disease therapy? *Trends Pharmacol Sci, 26*(7), 341-344. doi:10.1016/j.tips.2005.05.002

Merienne, N., Meunier, C., Schneider, A., Seguin, J., Nair, S. S., Rocher, A. B., . . . Deglon, N. (2019). Cell-Type-Specific Gene Expression Profiling in Adult Mouse Brain Reveals Normal and Disease-State Signatures. *Cell reports, 26*(9), 2477-2493 e2479. doi:10.1016/j.celrep.2019.02.003

Mestdagh, P., Hartmann, N., Baeriswyl, L., Andreasen, D., Bernard, N., Chen, C., . . . Vandesompele, J. (2014). Evaluation of quantitative miRNA expression platforms in the microRNA quality control (miRQC) study. *Nature methods, 11*(8), 809-815. doi:10.1038/nmeth.3014

Morimoto, K., Hooper, D. C., Carbaugh, H., Fu, Z. F., Koprowski, H., & Dietzschold, B. (1998). Rabies virus quasispecies: Implications for pathogenesis. *Proceedings of the National Academy of Sciences, 95*(6), 3152-3156. doi:10.1073/pnas.95.6.3152

Naldini, L., Blomer, U., Gallay, P., Ory, D., Mulligan, R., Gage, F. H., . . . Trono, D. (1996). In Vivo Gene Delivery and Stable Transduction of Nondividing Cells by a Lentiviral Vector. *Science, 272*(5259), 263-267. doi:10.1126/science.272.5259.263

Nash, K., Chen, W., & Muzyczka, N. (2008). Complete In Vitro Reconstitution of Adeno-Associated Virus DNA Replication Requires the Minichromosome Maintenance Complex Proteins. *Journal of virology, 82*(3), 1458-1464. doi:10.1128/jvi.01968-07

Nayak, R., & Pintel, D. J. (2007). Adeno-Associated Viruses Can Induce Phosphorylation of eIF2α via PKR Activation, Which Can Be Overcome by Helper Adenovirus Type 5 Virus-Associated RNA. *Journal of virology, 81*(21), 11908-11916. doi:10.1128/jvi.01132-07

Negrini, M., Wang, G., Heuer, A., Bjorklund, T., & Davidsson, M. (2020). AAV Production Everywhere: A Simple, Fast, and Reliable Protocol for In-house AAV Vector Production Based on Chloroform Extraction. *Curr Protoc Neurosci, 93*(1), e103. doi:10.1002/cpns.103

Nikolic, J., Belot, L., Raux, H., Legrand, P., Gaudin, Y., & A. Albertini, A. (2018). Structural basis for the recognition of LDL-receptor family members by VSV glycoprotein. *Nature communications, 9*(1). doi:10.1038/s41467-018-03432-4

Nonomura, S., Nishizawa, K., Sakai, Y., Kawaguchi, Y., Kato, S., Uchigashima, M., . . . Kimura, M. (2018). Monitoring and Updating of Action Selection for Goal-Directed Behavior through the Striatal Direct and Indirect Pathways. *Neuron, 99*(6), 1302-1314.e1305. doi:10.1016/j.neuron.2018.08.002

O'Callaghan, C., Bertoux, M., & Hornberger, M. (2013). Beyond and below the cortex: the contribution of striatal dysfunction to cognition and behaviour in neurodegeneration. *Journal of Neurology, Neurosurgery & Psychiatry, 85*(4), 371-378. doi:10.1136/jnnp-2012-304558

O'Carroll, D., & Schaefer, A. (2012). General Principals of miRNA Biogenesis and Regulation in the Brain. *Neuropsychopharmacology, 38*(1), 39-54. doi:10.1038/npp.2012.87

Oorschot, D. E. (1996). Total number of neurons in the neostriatal, pallidal, subthalamic, and substantia nigral nuclei of the rat basal ganglia: A stereological study using the cavalieri and optical disector methods. *The Journal of Comparative Neurology, 366*(4), 580-599. doi:10.1002/(sici)1096-9861(19960318)366:4<580::Aid-cne3>3.0.Co;2-0

Packer, A. N., Xing, Y., Harper, S. Q., Jones, L., & Davidson, B. L. (2008). The Bifunctional microRNA miR-9/miR-9* Regulates REST and CoREST and Is Downregulated in Huntington's Disease. *Journal of Neuroscience, 28*(53), 14341-14346. doi:10.1523/jneurosci.2390-08.2008

Pancho, A., Aerts, T., Mitsogiannis, M. D., & Seuntjens, E. (2020). Protocadherins at the Crossroad of Signaling Pathways. *Frontiers in Molecular Neuroscience, 13*. doi:10.3389/fnmol.2020.00117

Patil, K. S., Basak, I., Dalen, I., Hoedt, E., Lange, J., Lunde, K. A., . . . Møller, S. G. (2019). Combinatory microRNA serum signatures as classifiers of Parkinson's disease. *Parkinsonism & Related Disorders, 64*, 202-210. doi:10.1016/j.parkreldis.2019.04.010

Perreault, M. L., Hasbi, A., Alijaniaram, M., Fan, T., Varghese, G., Fletcher, P. J., . . . George, S. R. (2010). The Dopamine D1-D2 Receptor Heteromer Localizes in Dynorphin/Enkephalin Neurons. *Journal of Biological Chemistry, 285*(47), 36625-36634. doi:10.1074/jbc.M110.159954

Petri, R., Malmevik, J., Fasching, L., Åkerblom, M., & Jakobsson, J. (2014). miRNAs in brain development. *Experimental Cell Research, 321*(1), 84-89. doi:10.1016/j.yexcr.2013.09.022

Petri, R., Pircs, K., Jonsson, M. E., Akerblom, M., Brattas, P. L., Klussendorf, T., & Jakobsson, J. (2017). let-7 regulates radial migration of new-born neurons through positive regulation of autophagy. *The EMBO journal, 36*(10), 1379-1391. doi:10.15252/embj.201695235

Pfeffer, S., Sewer, A., Lagos-Quintana, M., Sheridan, R., Sander, C., Grässer, F. A., . . . Tuschl, T. (2005). Identification of microRNAs of the herpesvirus family. *Nature methods, 2*(4), 269-276. doi:10.1038/nmeth746

Pfister, E. L., DiNardo, N., Mondo, E., Borel, F., Conroy, F., Fraser, C., . . . Aronin, N. (2018). Artificial miRNAs Reduce Human Mutant Huntingtin Throughout the Striatum in a Transgenic Sheep Model of Huntington's Disease. *Human gene therapy, 29*(6), 663-673. doi:10.1089/hum.2017.199

Pilder, S., Moore, M., Logan, J., & Shenk, T. (1986). The adenovirus E1B-55K transforming polypeptide modulates transport or cytoplasmic stabilization of viral and host cell mRNAs. *Molecular and cellular biology, 6*(2), 470-476. doi:10.1128/mcb.6.2.470

Poelmans, G., Franke, B., Pauls, D. L., Glennon, J. C., & Buitelaar, J. K. (2013). AKAPs integrate genetic findings for autism spectrum disorders. *Translational Psychiatry, 3*(6), e270-e270. doi:10.1038/tp.2013.48

Poznansky, M., Lever, A., Bergeron, L., Haseltine, W., & Sodroski, J. (1991). Gene transfer into human lymphocytes by a defective human immunodeficiency virus type 1 vector. *Journal of virology, 65*(1), 532-536. doi:10.1128/JVI.65.1.532-536.1991

Rajman, M., & Schratt, G. (2017). MicroRNAs in neural development: from master regulators to fine-tuners. *Development, 144*(13), 2310-2322. doi:10.1242/dev.144337

Ralph, R. J., & Caine, S. B. (2005). Dopamine D1 and D2 Agonist Effects on Prepulse Inhibition and Locomotion: Comparison of Sprague-Dawley Rats to Swiss-Webster, 129X1/SvJ, C57BL/6J, and DBA/2J Mice. *Journal of Pharmacology and Experimental Therapeutics, 312*(2), 733-741. doi:10.1124/jpet.104.074468

Rashid, A. J., So, C. H., Kong, M. M. C., Furtak, T., El-Ghundi, M., Cheng, R., . . . George, S. R. (2006). D1-D2 dopamine receptor heterooligomers with unique pharmacology are coupled to rapid activation of Gq/11 in the striatum. *Proceedings of the National Academy of Sciences, 104*(2), 654-659. doi:10.1073/pnas.0604049104

Reed, E. R., Latourelle, J. C., Bockholt, J. H., Bregu, J., Smock, J., Paulsen, J. S., & Myers, R. H. (2018). MicroRNAs in CSF as prodromal biomarkers for Huntington disease in the PREDICT-HD study. *Neurology, 90*(4), e264-e272. doi:10.1212/wnl.0000000000004844

Reed, S. E., Staley, E. M., Mayginnes, J. P., Pintel, D. J., & Tullis, G. E. (2006). Transfection of mammalian cells using linear polyethylenimine is a simple and effective means of producing recombinant adeno-associated virus vectors. *Journal of virological methods, 138*(1-2), 85-98. doi:10.1016/j.jviromet.2006.07.024

Rehwinkel, J. (2005). A crucial role for GW182 and the DCP1:DCP2 decapping complex in miRNA-mediated gene silencing. *RNA, 11*(11), 1640-1647. doi:10.1261/rna.2191905

Richardson, G. M., Lannigan, J., & Macara, I. G. (2015). Does FACS perturb gene expression? *Cytometry Part A, 87*(2), 166-175. doi:10.1002/cyto.a.22608

Robinson, M. D., McCarthy, D. J., & Smyth, G. K. (2009). edgeR: a Bioconductor package for differential expression analysis of digital gene expression data. *Bioinformatics, 26*(1), 139-140. doi:10.1093/bioinformatics/btp616

Robinson, M. D., & Oshlack, A. (2010). A scaling normalization method for differential expression analysis of RNA-seq data. *Genome biology, 11*(3), R25. doi:10.1186/gb-2010-11-3-r25

Roos, R. A. C. (2010). Huntington's disease: a clinical review. *Orphanet Journal of Rare Diseases, 5*(1). doi:10.1186/1750-1172-5-40

Rosenblatt, A., Kumar, B. V., Mo, A., Welsh, C. S., Margolis, R. L., & Ross, C. A. (2012). Age, CAG repeat length, and clinical progression in Huntington's disease. *Movement Disorders, 27*(2), 272-276. doi:10.1002/mds.24024

Roser, A. E., Caldi Gomes, L., Schünemann, J., Maass, F., & Lingor, P. (2018). Circulating miRNAs as Diagnostic Biomarkers for Parkinson's Disease. *Frontiers in Neuroscience, 12*. doi:10.3389/fnins.2018.00625

Rueden, C. T., Schindelin, J., Hiner, M. C., DeZonia, B. E., Walter, A. E., Arena, E. T., & Eliceiri, K. W. (2017). ImageJ2: ImageJ for the next generation of scientific image data. *BMC bioinformatics, 18*(1), 529. doi:10.1186/s12859-017-1934-z

Salmon, P., & Trono, D. (2007). Production and Titration of Lentiviral Vectors. *Current Protocols in Human Genetics, 54*(1). doi:10.1002/0471142905.hg1210s54

Samulski, R. J., Berns, K. I., Tan, M., & Muzyczka, N. (1982). Cloning of adeno-associated virus into pBR322: rescue of intact virus from the recombinant plasmid in human cells. *Proceedings of the National Academy of Sciences, 79*(6), 2077-2081. doi:10.1073/pnas.79.6.2077

Samulski, R. J., & Muzyczka, N. (2014). AAV-Mediated Gene Therapy for Research and Therapeutic Purposes. *Annual Review of Virology, 1*(1), 427-451. doi:10.1146/annurev-virology-031413-085355

Santini, E., Heiman, M., Greengard, P., Valjent, E., & Fisone, G. (2009). Inhibition of mTOR signaling in Parkinson's disease prevents L-DOPA-induced dyskinesia. *Sci Signal, 2*(80), ra36. doi:10.1126/scisignal.2000308

Sanuki, R., Onishi, A., Koike, C., Muramatsu, R., Watanabe, S., Muranishi, Y., . . . Furukawa, T. (2011). miR-124a is required for hippocampal axogenesis and retinal cone survival through Lhx2 suppression. *Nature Neuroscience, 14*(9), 1125-1134. doi:10.1038/nn.2897

Sayeg, M. K., Weinberg, B. H., Cha, S. S., Goodloe, M., Wong, W. W., & Han, X. (2015). Rationally Designed MicroRNA-Based Genetic Classifiers Target Specific Neurons in the Brain. *ACS Synthetic Biology, 4*(7), 788-795. doi:10.1021/acssynbio.5b00040

Schaefer, A., O'Carroll, D. n., Tan, C. L., Hillman, D., Sugimori, M., Llinas, R., & Greengard, P. (2007). Cerebellar neurodegeneration in the absence of microRNAs. *Journal of Experimental Medicine, 204*(7), 1553-1558. doi:10.1084/jem.20070823

Scheschonka, A., Dessauer, C. W., Sinnarajah, S., Chidiac, P., Shi, C.-S., & Kehrl, J. H. (2000). RGS3 Is a GTPase-Activating Protein for Giα and Gqα and a Potent Inhibitor of Signaling by GTPase-Deficient Forms of Gqα and G11α. *Molecular pharmacology, 58*(4), 719-728. doi:10.1124/mol.58.4.719

Schindelin, J., Arganda-Carreras, I., Frise, E., Kaynig, V., Longair, M., Pietzsch, T., . . . Cardona, A. (2012). Fiji: an open-source platform for biological-image analysis. *Nature methods, 9*(7), 676-682. doi:10.1038/nmeth.2019

Schulz, J., Takousis, P., Wohlers, I., Itua, I. O. G., Dobricic, V., Rücker, G., . . . Lill, C. M. (2019). Meta-analyses identify differentially expressed microRNAs in Parkinson's disease. *Annals of Neurology, 85*(6), 835-851. doi:10.1002/ana.25490

Schüitze, K., & Lahr, G. (1998). Identification of expressed genes by laser-mediated manipulation of single cells. *Nature Biotechnology, 16*(8), 737-742. doi:10.1038/nbt0898-737

Sebastianutto, I., Goyet, E., Andreoli, L., Font-Ingles, J., Moreno-Delgado, D., Bouquier, N., . . . Perroy, J. (2020). D1-mGlu5 heteromers mediate noncanonical dopamine signaling in Parkinson's disease. *Journal of Clinical Investigation, 130*(3), 1168-1184. doi:10.1172/jci126361

Senapathy, P., Tratschin, J.-D., & Carter, B. J. (1984). Replication of adeno-associated virus DNA. *Journal of Molecular Biology, 179*(1), 1-20. doi:10.1016/0022-2836(84)90303-6

Shen, M. Y. F., Perreault, M. L., Bambico, F. R., Jones-Tabah, J., Cheung, M., Fan, T., . . . George, S. R. (2015). Rapid anti-depressant and anxiolytic actions following dopamine D1–D2 receptor heteromer inactivation. *European Neuropsychopharmacology, 25*(12), 2437-2448. doi:10.1016/j.euroneuro.2015.09.004

Sheth, U. (2003). Decapping and Decay of Messenger RNA Occur in Cytoplasmic Processing Bodies. *Science, 300*(5620), 805-808. doi:10.1126/science.1082320

Shibata, M., Nakao, H., Kiyonari, H., Abe, T., & Aizawa, S. (2011). MicroRNA-9 Regulates Neurogenesis in Mouse Telencephalon by Targeting Multiple Transcription Factors. *Journal of Neuroscience, 31*(9), 3407-3422. doi:10.1523/jneurosci.5085-10.2011

Simonetti, M., Paldy, E., Njoo, C., Bali, K. K., Worzfeld, T., Pitzer, C., . . . Kuner, R. (2019). The impact of Semaphorin 4C/Plexin-B2 signaling on fear memory via remodeling of neuronal and synaptic morphology. *Molecular Psychiatry, 26*(4), 1376-1398. doi:10.1038/s41380-019-0491-4

Solis, O., Garcia-Montes, J. R., Gonzalez-Granillo, A., Xu, M., & Moratalla, R. (2015). Dopamine D3 Receptor Modulates l-DOPA-Induced Dyskinesia by Targeting D1 Receptor-Mediated Striatal Signaling. *Cerebral cortex*. doi:10.1093/cercor/bhv231

Sonntag, F., Kother, K., Schmidt, K., Weghofer, M., Raupp, C., Nieto, K., . . . Kleinschmidt, J. A. (2011). The Assembly-Activating Protein Promotes Capsid Assembly of Different Adeno-Associated Virus Serotypes. *Journal of virology, 85*(23), 12686-12697. doi:10.1128/jvi.05359-11

Stanley, G., Gokce, O., Malenka, R. C., Sudhof, T. C., & Quake, S. R. (2020). Continuous and Discrete Neuron Types of the Adult Murine Striatum. *Neuron, 105*(4), 688-699 e688. doi:10.1016/j.neuron.2019.11.004

Stracker, T. H., Cassell, G. D., Ward, P., Loo, Y.-M., van Breukelen, B., Carrington-Lawrence, S. D., . . . Weitzman, M. D. (2004). The Rep Protein of Adeno-Associated Virus Type 2 Interacts with Single-Stranded DNA-Binding Proteins That Enhance Viral Replication. *Journal of virology, 78*(1), 441-453. doi:10.1128/jvi.78.1.441-453.2004

Sun, G., Ye, P., Murai, K., Lang, M.-F., Li, S., Zhang, H., . . . Shi, Y. (2011). miR-137 forms a regulatory loop with nuclear receptor TLX and LSD1 in neural stem cells. *Nature communications, 2*(1). doi:10.1038/ncomms1532

Sun, X., Lu, Y., Bish, L. T., Calcedo, R., Wilson, J. M., & Gao, G. (2010). Molecular Analysis of Vector Genome Structures After Liver Transduction by Conventional and Self-Complementary Adeno-Associated Viral Serotype Vectors in Murine and Nonhuman Primate Models. *Human gene therapy, 21*(6), 750-761. doi:10.1089/hum.2009.214

Tecuapetla, F., Jin, X., Lima, S. Q., & Costa, R. M. (2016). Complementary Contributions of Striatal Projection Pathways to Action Initiation and Execution. *Cell, 166*(3), 703-715. doi:10.1016/j.cell.2016.06.032

Tervo, D. Gowanlock R., Hwang, B.-Y., Viswanathan, S., Gaj, T., Lavzin, M., Ritola, Kimberly D., . . . Karpova, Alla Y. (2016). A Designer AAV Variant Permits Efficient Retrograde Access to Projection Neurons. *Neuron, 92*(2), 372-382. doi:10.1016/j.neuron.2016.09.021

Toledo, J. R., Prieto, Y., Oramas, N., & Sanchez, O. (2009). Polyethylenimine-based transfection method as a simple and effective way to produce recombinant lentiviral vectors. *Applied biochemistry and biotechnology, 157*(3), 538-544. doi:10.1007/s12010-008-8381-2

Trono, D. (2000). Lentiviral vectors: turning a deadly foe into a therapeutic agent. *Gene therapy, 7*(1), 20-23. doi:10.1038/sj.gt.3301105

Ueda, Y., Yamanaka, K., Noritake, A., Enomoto, K., Matsumoto, N., Yamada, H., . . . Kimura, M. (2017). Distinct Functions of the Primate Putamen Direct and Indirect Pathways in Adaptive Outcome-Based Action Selection. *Frontiers in Neuroanatomy, 11*. doi:10.3389/fnana.2017.00066

Vallès, A., Evers, M. M., Stam, A., Sogorb-Gonzalez, M., Brouwers, C., Vendrell-Tornero, C., . . . Konstantinova, P. (2021). Widespread and sustained target engagement in Huntington's disease minipigs upon intrastriatal microRNA-based gene therapy. *Science Translational Medicine, 13*(588). doi:10.1126/scitranslmed.abb8920

van den Brink, S. C., Sage, F., Vértesy, Á., Spanjaard, B., Peterson-Maduro, J., Baron, C. S., . . . van Oudenaarden, A. (2017). Single-cell sequencing reveals dissociation-induced gene expression in tissue subpopulations. *Nature methods, 14*(10), 935-936. doi:10.1038/nmeth.4437

Viney, L., Bürckstümmer, T., Eddington, C., Mietzsch, M., Choudhry, M., Henley, T., . . . Parrish, C. R. (2021). Adeno-associated Virus (AAV) Capsid Chimeras with Enhanced Infectivity Reveal a Core Element in the AAV Genome Critical for both Cell Transduction and Capsid Assembly. *Journal of virology, 95*(7). doi:10.1128/jvi.02023-20

Vonsattel, J.-P., Myers, R. H., Stevens, T. J., Ferrante, R. J., Bird, E. D., & Richardson, E. P. (1985). Neuropathological Classification of Huntington's Disease. *Journal of Neuropathology and Experimental Neurology, 44*(6), 559-577. doi:10.1097/00005072-198511000-00003

Wirdefeldt, K., Adami, H. O., Cole, P., Trichopoulos, D., & Mandel, J. (2011). Epidemiology and etiology of Parkinson's disease: a review of the evidence. *Eur J Epidemiol, 26 Suppl 1*, S1-58. doi:10.1007/s10654-011-9581-6

Wistuba, A., Kern, A., Weger, S., Grimm, D., & Kleinschmidt, J. A. (1997). Subcellular compartmentalization of adeno-associated virus type 2 assembly. *Journal of virology, 71*(2), 1341-1352.

Xiao, X., Li, J., & Samulski, R. J. (1998). Production of high-titer recombinant adeno-associated virus vectors in the absence of helper adenovirus. *Journal of virology, 72*(3), 2224-2232. doi:10.1128/JVI.72.3.2224-2232.1998

Yaguchi, M., Ohashi, Y., Tsubota, T., Sato, A., Koyano, K. W., Wang, N., & Miyashita, Y. (2013). Characterization of the properties of seven promoters in the motor cortex of rats and monkeys after lentiviral vector-mediated gene transfer. *Hum Gene Ther Methods, 24*(6), 333-344. doi:10.1089/hgtb.2012.238

Zalocusky, K. A., Ramakrishnan, C., Lerner, T. N., Davidson, T. J., Knutson, B., & Deisseroth, K. (2016). Nucleus accumbens D2R cells signal prior outcomes and control risky decision-making. *Nature, 531*(7596), 642-646. doi:10.1038/nature17400

Zhao, C., Sun, G., Li, S., Lang, M.-F., Yang, S., Li, W., & Shi, Y. (2010). MicroRNA let-7b regulates neural stem cell proliferation and differentiation by targeting nuclear receptor TLX signaling. *Proceedings of the National Academy of Sciences, 107*(5), 1876-1881. doi:10.1073/pnas.0908750107

Zhao, C., Sun, G., Li, S., & Shi, Y. (2009). A feedback regulatory loop involving microRNA-9 and nuclear receptor TLX in neural stem cell fate determination. *Nature structural & molecular biology, 16*(4), 365-371. doi:10.1038/nsmb.1576

Zhu, J. J., Qin, Y., Zhao, M., Van Aelst, L., & Malinow, R. (2002). Ras and Rap Control AMPA Receptor Trafficking during Synaptic Plasticity. *Cell, 110*(4), 443-455. doi:10.1016/s0092-8674(02)00897-8

Zufferey, R., Dull, T., Mandel, R. J., Bukovsky, A., Quiroz, D., Naldini, L., & Trono, D. (1998). Self-inactivating lentivirus vector for safe and efficient in vivo gene delivery. *Journal of virology, 72*(12), 9873-9880.

Zufferey, R., Nagy, D., Mandel, R. J., Naldini, L., & Trono, D. (1997). Multiply attenuated lentiviral vector achieves efficient gene delivery in vivo. *Nature Biotechnology, 15*(9), 871-875. doi:10.1038/nbt0997-871

Zuiderveld, K. (1994). Contrast limited adaptive histogram equalization. In *Graphics gems IV* (pp. 474–485): Academic Press Professional, Inc.

Acknowledgements

I would like to begin by thanking my supervisor Cilla for the work she put in and for doing her best to constantly encourage me, despite the numerous setbacks. I am aware it can be straining to deal with someone as consistently pessimistic as myself and for never losing faith or letting any negative emotions seep through, I thank you.

Secondly, I would like to extend a thank you to Luis who has similarly kept me company as the only other permanent member of our small group throughout my time here. You have provided me with a wealth of knowledge and good advice many times and without your help I would doubtless be in a worse position than I am today. Your company outside of work has also been greatly appreciated and I wish you, Aurelie, Inês, and Léa only the best for the future.

I want to continue by thanking Dorothee and Martin, my student's, whom I hope to have taught something useful. I expect none of them will read this, but you both helped me become a better teacher and for that I am grateful.

Continuing the trend of thanking people who will most likely not read it, I would like to thank two former members of our group, Christina and Lu. Christina you were always helpful and took the time to help me when I had just started and was completely lost. Similarly, Lu, thank you for your patience with me, even when I was being insufferable.

To switch it up I would like to thank some people who will probably actually read it. Marcus, aka. Mr Davidsson. First of all, thank you for spelling your name the only correct way to spell Marcus. Most other Marcuses that I know did not have this basic decency. Second, thank you for all your advice the last few years. You have been one of the people I have been able to rely on professionally and you have always been a joy to converse with. Should our paths not cross again in the future I wish you fortune and many sunny golf-filled days.

I am going to continue by thanking Tomas for many interesting discussions at journal club and always happy to give advice regarding AAVs. Without yours and Marcus' help I don't know if I would have been able to do all of the AAV stuff I actually ended up doing. I would also like to thank Andy for his advice, especially these last few months.

I hope everything works out for you and that I've been able to give something back in return for what I've gotten.

Jenny and Ulla, I want to thank you for being helpful and friendly and allowing me to bombard you with questions regarding your respective areas of expertise sometimes. Similarly, I'd like to thank Marie, Micke, Elsy, and Susanne for being lovely and helpful people and doing their best to help make my work easier.

In addition to thanking Rebecca, Raquel, and Johan who provided valuable input or advice on work that did make it into this thesis, I also want to thank Anna, Isak and Ale for providing me with cells, advice or help for projects that didn't.

I would like to thank the, over the years many, many people, who have worked at A11 and either helped with work in some way or provided company in the fika-room. Apart from the people I have already mentioned, current residents Elin, Abdullah, Pia, Marie, Malin, Bengt, Chris, Diahann, Yoghita, Fredrik, Jessica, Mette, Janko, Janitha, Shelby, Edo, Sol, Jenny, Paulina, Petter, Ana, Eliska, Susanne, Esbjörn, Apostolos, Jan, Fredrik, Andreas, Sara, and Anita thank you for keeping A11 great these last few weeks, months and for some of you, years. Finally, I would like to thank all my former colleagues and fellow A11ers who have provided valuable scientific input and been willing to share their knowledge, in addition to making A11 a more enjoyable place to work.